

P-1693



# Modeling and Analysis of Solidification Process in Sand Casting



A Project Report

*Submitted by*



**E.Karthikeyan - 71204402005**

*in partial fulfillment for the award of the degree  
of*

**Master of Engineering  
in  
CAD/CAM**

**DEPARTMENT OF MECHANICAL ENGINEERING  
KUMARAGURU COLLEGE OF TECHNOLOGY  
COIMBATORE - 641 006**

**ANNA UNIVERSITY :: CHENNAI 600 025**

# ANNA UNIVERSITY :: CHENNAI 600 025

## BONAFIDE CERTIFICATE

Certified that this project report entitled "Modeling and Analysis of Solidification Process in Sand Casting" is the bonafide work of

Mr. E.Karthikeyan

-

Register No. 71204402005

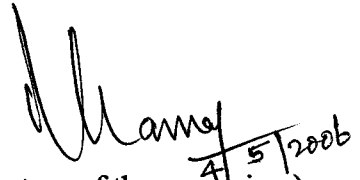
Who carried out the project work under my supervision.



(Signature of the HOD)

**Dr. T. P. MANI**

HEAD OF THE DEPARTMENT



(Signature of the supervisor)

**Mr. T.KANNAN**

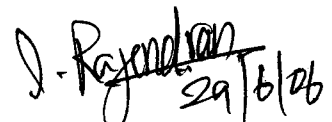
ASSISTANT PROFESSOR



Internal Examiner

**Dr. T.P. Mani**

B.E., M.E., Ph.D., DML., MIE., MNIOR., MISTE.,  
Dean & HoD / Dept. of Mech. Engg.  
Kumaraguru College of Technology  
Coimbatore - 641 006



External Examiner

**DEPARTMENT OF MECHANICAL ENGINEERING  
KUMARAGURU COLLEGE OF TECHNOLOGY**

**COIMBATORE 641 006**

Second National Conference on

# ADVANCES IN MANUFACTURING AND RESOURCE ANALYSIS

(A systematic approach to improve quality and productivity)

Department of Mechanical Engineering

## PSNA COLLEGE OF ENGINEERING AND TECHNOLOGY

Kothandaraman Nagar, Dindigul 624 622

# AMARA 2006

# CERTIFICATE

This is to certify that Mr./AAs. E. KARTHIKEYAN

KUMARASURU COLLEGE OF TECHNOLOGY, COMBATORES

has

participated in two days Second National Conference on Advances in Manufacturing and Resource

Analysis AMARA 2006 (A systematic approach to improve quality and productivity) conducted by

Department of Mechanical Engineering, on 21<sup>st</sup> and 22<sup>nd</sup> April 2006 and presented a paper on

MODELING AND ANALYSIS OF SOLIDIFICATION PROCESS IN SAND CASTING

*A. V. Arudhraman*  
Organizing Secretary

*Arum*

Head of the Department

Chairman



Estd : 1984

Kothandaraman  
Nagar

## **ABSTRACT**

Sand casting is one of the basic manufacturing processes, involves considerable metallurgical and mechanical aspects. Sand casting can yield results that are as fine and true to detail as any other casting method. Hence properly designed mould and good control over the process parameters are must for quality castings. Computer simulation procedure based process development can be used for rapid process development in a shorter time. Such a computer simulation based procedure, often use FINITE ELEMENT ANALYSIS based software systems, which can improve the quality and enhance productivity of the enterprise by way of faster development of new product.

In this project (i) A computer program is developed to model the solidification process of metals, using explicit finite difference method. Using the model, Simulation of solidification of metal and sand mold are done and (ii) validating the result of simulation, by comparing with the analysis results and experimental literature. Numerical simulation of solidification is useful in getting high quality castings and minimizing product cost and scrap. The analysis is made using Ansys 8.1. The change of temperature in the casting and sand with time was monitored. Interpretation of results, used to optimize the parameters, so that it is easy to evaluate the defects such as shrinkage porosities, cold shut, hot tears and so on improve the quality of casting.

## ஆய்வுச் சுருக்கம்

மணல் வார்ப்பு என்பது அடிப்படை உற்பத்தி முறைகளில் ஒன்றாகும். மற்ற முறைகளை விட மணல் வார்ப்பு முறை மூலம் மிகத் துல்லியமான வார்ப்பைப் பெறலாம். மணல் வார்ப்பு முறை மூலம் மிகப்பெரிய பாகங்களை உருவாக்க முடியும். (இரும்பு, வெண்கலம், பித்தளை மற்றும் அலுமினியம்) கணினி மாதிரி முறை மூலம் மிகக் குறுகிய காலத்தில் விரைவாகப் பதில்களைப் பெறமுடியும். மென் பொருளில் உள்ள பெனைட் எலிமென்ட் பகுப்பாய்வினை பயன்படுத்தி குறைந்த விலையில் உயர்ந்த தரமுடைய பொருள்களை உற்பத்தி செய்ய உதவியாக இருக்கும்.

தற்போதைய ஆராய்ச்சியின் குறிக்கோள் (i) கணினி முறை மூலம் விளக்கமான முறையில் உலோகங்கள் மற்றும் உலோகக் கலவையின் மாதிரியை உருவாக்குதல், இம்முறையைப் பயன்படுத்தி அலுமினியம் - சிலிகன் கலவையை உலோக மற்றும் மணல் வார்ப்பு முறை மூலம் உறைய வைத்தல் (ii) இறுதியாக இம்முறையை பிரித்து நமக்கு கிடைத்த விபரங்களை முன்பு பதிவு செய்துள்ள அறிக்கையுடன் ஒப்பிடுதல். பின்ன மாதிரி வார்ப்பு முறை மூலம் உயர் தரமுடைய வார்ப்பு சேதாரமின்றி பெறப்படுகிறது. மேலும் இவ்வார்ப்பு முறையில் உற்பத்தி செலவும் குறைவு. இவ்வாய்வு முறையில் ஏற்படும் வெப்ப மாற்றம் மற்றும் குறிப்பிட்ட நேரத்தில் எடுக்கப்படும் மணல் கணக்கிடப்படுகிறது. முடிவுகளை அலசி தாதுப்பொருள் குறைபாடு மற்றம் தரக் குறைபாட இவற்றை நீக்கி வார்ப்பின் தரத்தை உயர்த்த முடியும்.

## **ACKNOWLEDGEMENT**

The author ever indebted to his guide **Mr.T.Kannan**, Assistant Professor, Department of Mechanical Engineering, Kumaraguru College of Technology, Coimbatore for his excellent, utmost motivation, valuable advice, untiring support, timely suggestion, constant encouragement, enthusiasm, relentless patience, and inspiration throughout the study, holding us in all the places we faltered.

The author express his humble gratitude to **Dr.T.P.Mani**, Head of the Department, Mechanical Engineering, Kumaraguru College of Technology, Coimbatore for facilitating conditions for carrying out the research work smoothly.

The author wish to express his deep sense of reverential gratitude to **Dr.K.K.Padmanabhan**, Principal, Kumaraguru College of Technology, Coimbatore, for providing the facilities to conduct this study.

At the outset, the author would like to thank **Dr.N.Gunasekaran**, Department of Mechanical Engineering, Kumaraguru College of Technology, Coimbatore who has given me this opportunity to undergo this research work successfully.

The author also wish to thank **Mr.Sriharan**, and **Mr.N.Sivakumar**, Technician, CAD lab for being with us throughout this venture, right from the scratch and helping us in completing the project successfully.

The author owes his sincere thanks to all elders, parents, teachers and Lord Almighty who have bestowed upon their generous blessings in all endeavors.

# CONTENTS

<b>Title</b>	<b>Page No.</b>
Certificate	i
Abstract	iii
Acknowledgement	v
Contents	vi
List of Tables	ix
List of Figures	x
List of Symbols and Abbreviations	xii
<b>CHAPTER 1 INTRODUCTION</b>	2
<b>CHAPTER 2 LITERATURE REVIEW</b>	5
<b>CHAPTER 3 SAND CASTING</b>	
3.1 Introduction	9
3.2 Solidification Process in Casting	10
3.2.1 Causes of Solidification Defects	14
<b>CHAPTER 4 CASTING GEOMETRY</b>	
4.1 Introduction	16
4.2 Casting composition	16
4.3 Experimental Results	
4.3.1 Introduction	18
4.3.2 Experimental Procedure	18
4.3.3 Results	19

## **CHAPTER 5 DEVELOPMENT OF NODE EQUATIONS**

5.1	Introduction	23
5.2	General Node	23
5.3	Corner Node	24
5.4	Stability of the Approximations	26
5.5	Initial Temperature Distribution	27
5.5.1	None of the Metal Solidifies	28
5.5.2	All of the Metal Solidifies	28
5.5.3	The Metal Partly Solidifies	29

## **CHAPTER 6 COMPUTATIONAL METHOD**

6.1	Introduction to ANSYS 8.1	32
6.2	Ansys Limits	32
6.3	Approach and Assumptions	33
6.4	Summary of Steps	33
6.5	Preparation for Thermal Analysis	
6.5.1	Setting the Preferences.	35
6.5.2	Reading the Geometry of the Casting.	35
6.5.3	Defining Material Properties.	35
6.5.4	Defining the Element Type.	39
6.5.5	Meshing the Model.	39
6.5.6	Applying Convection Loads On The Exposed Boundary Lines.	40
6.5.7	Defining the Analysis Type.	40
6.5.8	Specifying Initial Conditions for the Transient.	41
6.5.9	Setting the Time, Time Step Size, and Related Parameters.	41
6.5.10	Setting the Output Controls.	41
6.5.11	Solving the conditions.	41
6.5.12	Entering the Time-History Postprocessor and Define Variables.	42
6.5.13	Plotting Temperature Vs Time.	42
6.5.14	Animating the Results.	45



**CHAPTER 7 ALGORITHM AND FLOWCHART FOR  
THERMAL ANALYSIS**

7.1	Introduction	49
7.2	Algorithm	49
7.3	Flow chart	50
7.4	Input Nodal Values	52
7.5	Output Nodal Values	53

**CHAPTER 8 RESULTS AND DISCUSSIONS** 55

**CHAPTER 9 CONCLUSIONS** 59

**APPENDIX**

**REFERENCES** 65

## LIST OF TABLES

<b>Table</b>	<b>Title</b>	<b>Page No</b>
4.1	Typical properties for Aluminum	17
6.1	Ansys Limits	32
6.2	Density of Materials	36
6.3	Specific Heat for Sand	36
6.4	Thermal Conductivity for Sand	37
6.5	Thermal Conductivity for Aluminum	38
6.6	Specific Heat for Aluminum	38
6.7	Loads Applied	40
6.8	Initial Conditions	41

## LIST OF FIGURES

Figure	Title	Page No
3.1	(a) A Thick/Thin Section Casting Showing Tensile Stress in the Thick Section.	12
	(a) An Even Walled Casting Showing Internal Tensile Stresses.	13
3.2	Physical Mechanisms in Solidification	14
4.1	Casting Geometry	16
4.2	Temperature Measurements in Sand During Solidification and Cooling of Aluminum Casting.	19
4.3	Thermocouple Measurements of Cooling Curves In Experimental Casting of Aluminum.	20
4.4	Thermocouple Measurements of Cooling Curves in the Interface Region.	21
5.1	General Node and Its Associated Control Volume	23
5.2	Node and Control Volume Associated With The Corner of the Casting.	25
5.3	Control Volume Considered When Calculating The Initial Sand-Metal Interface Temperature.	27
6.1	Schematic Diagrams for Analysis of Casting.	34
6.2.	Geometry Input	35
6.3	Specific Heat Vs Temperature for Sand	36
6.4	Thermal Conductivity Vs Temperature for Sand	37
6.5	Thermal Conductivity Vs Temperature for Aluminum	38
6.6	Specific Heat Vs Temperature for Aluminum	39
6.7	Meshed Model	39
6.8	Convection Load On Top Of Geometry	40
6.9	Iteration	42
6.10	Temperature Vs Time for Metal	43

6.12	Temperature Vs Time for Sand	44
6.13	Temperature Distribution at 0.01 Hrs	45
6.14	Temperature Distribution at 0.52 Hrs	46
6.15	Temperature Distribution at 1.04 Hrs	46
6.16	Temperature Distribution at 2.075 Hrs	47
8.1	Temperature Distribution in Metal	55
8.2	Temperature Distribution in Interface Region	56
8.3	Temperature Distribution in Sand	57

## LIST OF SYMBOLS AND ABBREVIATIONS

Q	Heat Transfer Rate (Conduction) (Btu/hr)
U	Temperature ( $^{\circ}\text{F}$ )
$\Delta t$	Time (hr)
P	Density ( $\text{lb}/\text{ft}^3$ )
K	Thermal Conductivity
P	Density {Btu/(hr-ft- $^{\circ}\text{F}$ )}
$C_p$	Specific Heat {Btu/(lb- $^{\circ}\text{F}$ )}
M	Metal
S	Sand
Ss	Surrounding Nodes
I	Interface
C	Corner
i,j	Grid Positions
$T_{om}$	Initial Metal Temperature( $^{\circ}\text{F}$ )
$T_{os}$	Initial Sand Temperature( $^{\circ}\text{F}$ )
FS	Fraction Solidified
$T_{st}$	Temperature at Which Solidification ( $^{\circ}\text{F}$ )
$T_f$	Temperature at Which Solidification Is Completed ( $^{\circ}\text{F}$ )
$\theta$	Angle between the Liquidus and an Isotherm
$\phi$	Angle between the Solidus and an Isotherm

# *Chapter 1*

*Introduction*

The Computational Analysis is becoming increasingly important tool to understand and improve industrial processes, such as sand casting. Numerical simulation of solidification is useful in getting high quality castings and minimizing product cost and scrap. A proper understanding of solidification mechanism helps in avoiding major casting defects like shrinkage, porosity hot-tears, cracks distortions and poor mechanical properties.

The objectives of the present work are (i) Developing a computer Program to model the solidification process of metals and alloys, using explicit finite difference method. Using the model, simulate the solidification of Al-Si alloy in metal and sand mould and (ii) validating the result of simulation by comparing with the experimental findings and reported literature. The explicit difference approximation method divides space and time into discrete uniform subintervals and replaces time and space derivatives by finite difference approximations, permitting one to easily compute values of the function at a time  $\Delta t$  after the initial time.

The rate of cooling governs the microstructure to a large extent, which in turn controls the mechanical properties like strength, hardness, mach inability, etc. From realistic considerations, the experimental routes are always better for design and development of mould and for arriving at the optimum process parameters. It is costly and time consuming and may be impossible in some cases. But a computer simulation of the whole process is a convenient way of design of mould and analyzing the effect of various parameters. The field variables namely temperatures at all nodal points are varying with time. Also the thermal properties like thermal conductivity, density and specific heat are varying with temperature and hence a non-linear transient solution technique had been used. The input material properties are given with respect to the temperature. Some properties change as temperature changes. The load conditions considered in this are the convection loads and the initial temperature of metal and sand. During solidification from liquid to solid state, Aluminum alloy with long freezing range tend to develop casting defects like hot-tears and cracks. This happens during the stage of solidification when the solid dendrites while contracting are still not strong enough to overcome the hindrance offered by non-collapsible cores and

A computer program in C++ language has been developed to perform thermal analysis of two-dimensional solidifying bodies. Using this program the analysis can be made at different grid positions at an economical manner, compare to experimental and software results. The finite difference idealization has two groups of grids namely casting, mould grids. The capabilities of the program were dynamic memory allocation, incorporation of temperature dependent material properties, skyline storage of global matrices, Gaussian elimination method for solving, facility to edit the input data, facility to use stored material properties for certain materials. The program asks for the number of grids in the mesh and heat transfer coefficient. Thermal properties viz. conductivity and specific heat which is a function of temperature were given as input, and the load conditions are specified.

Ansys mechanical and Ansys multiphysics are self contained analysis tools incorporating pre-processing (geometry creation, meshing), solver and post processing modules in a unified graphical user interface. The software is used to analyze a broad range of applications. The software is used to analyze a broad range of applications. Ansys mechanical incorporates both structural and material non-linearities. Ansys multiphysics includes solvers for thermal, structural, cfd, electromagnetics, acoustics and can couple these separate physics together in order to address multi-disciplinary applications.

The results from Ansys 8.0, mathematical model and the experimental literature report are compared. The output is the graph drawn between temperature and time at different grid positions. Using the output, Solidification rate can be predicted and the type of structure at different grid points can be found from the temperature versus time graph.



# *Chapter 2*

*Literature Review*

**Sulaiman and Hamouda (2004)**, This paper describes simulation and experimental results of thermal analysis in sand casting process. Analysis is done by concentrating on chosen nodes as references. The change of temperature in the casting and sand with time was monitored. In comparing modeling with experimental results, the experimental temperature curves are generally higher than modeling for mold, this is because trapped air and porosity of the sand mold. Since the sand mold has a lot of air gaps, the temperature should be higher than expected in the simulation.

**Pehlke, Kirt, Marrone and Cook (1985)**, The heat transfer at the half-length plane was essentially 2-dimensional, was cast in Aluminium-silicon alloy using dried mold sand. A two-dimensional computer simulation was to investigate solidification at the central plane of a long, square bar casting. The comparisons between experimental and simulated results are compared. The freezing range of the metal cast had essentially no effect on the accuracy of the simulation. Excellent agreement was obtained between thermocouple measurements on the solidifying casting and the computer simulation using independently determined material thermal properties.

**Venkatesan, Gopinath and Rajadurai (2005)**, A computer program is developed to model the solidification process of metals and alloys. A C++ code is developed for the simulation of casting solidification gives temperature distribution in nodes at various time intervals. The program can perform two dimensional heat transfer analysis for non-linear transient cases. Latent heat is incorporated in this program using enthalpy method. Taking these temperatures as input, this program can calculate values of  $G$ ,  $R$ ,  $(dT/dt)$ . From these values grain structure can be found. Programme is to be extended for pre and post processing to take the input for the program and for giving graphical output respectively.

**Carter, Cox, Gandin and Reed (2000)**, A process model is described for the grain selection occurring during solidification of single crystal investment castings, which are now widely used for a number of critical applications in gas turbine engines. The model is used to study the geometrical factors influencing competitive growth of two designs of grain selector, and in particular the conferral of any control of the secondary orientation. Evolutions of grain size, grain texture, and distribution of casting orientation are determined.

**Lan, Lin and Hsu (2001)**, An adaptive finite volume method is presented for solving incompressible heat flow problems with an unknown mesh-solid interface, mainly in solidification applications, using primitive variables on a fixed collocated grid. Extensive tests are performed for cases with a fixed or free interface, and excellent agreement with the body fitted or front tracking schemes. The present approach is particularly suitable for problems having a complicated interface morphology as well as phase evolution, such as the phase field simulation of dendritic growth.

**Majchrzak and Mendakiewicz (1995)**, Here casting-mold environment is analyzed. Composition of FEM (casting) & BEM (mold). Calculations of temperature field, kinematics of solidification, solidification time. Solution of matrix equation allows determining the enthalpy-temperature field in casting and molding sub domains.

**Jeong and Yang (2001)**, an adaptive grid refinement technique is incorporated in the volume of the fluid and the marker surface methods for three dimensional finite element analysis of the filling stage in the die casting process. The numerical results have been in good agreement with the experimental results. the flow patterns obtained by using the adaptive grid have represented the flow phenomenon in amore detailed manner than those obtained by using the fixed grid.

**Licetal (2001)**, study the development of thermal stress and to predict the hot tearing and residual stress of shaped, two models were used to carry out the stress analysis of two stages of solidification. Finite element method to simulate the heat transfer process accompanying the solidification process is discussed. Further simulation of the shrinkage and the thermal stresses using finite element methods is also discussed.

**Jinho lee (1994)**, investigated the thermal stresses in a solidifying body during vertical solidification of a pure metal with solid liquid density change have been analyzed by a finite volume method / finite element method.

# *Chapter 3*

## *Sand Casting*

### 3.1 INTRODUCTION

Casting is the oldest known process to produce metallic components. The first metal casting was done using stone and metal moulds during the period of 4000–3000 BC. Since then, various casting processes have been developed. In casting, the liquid material is poured into a cavity (die or mould) corresponding to the desired geometry. The shape obtained in the liquid material is now stabilized, usually by solidification, and can be removed from the cavity as a solid component. One of the oldest casting methods is sand casting. Sand casting is a widely used method of producing rough metal castings. Unfinished, these castings have an easily recognizable, grainy texture, although most foundries will perform finishing services that yield a smoother surface.

Sand castings are made by first starting with a wood or metal representation of the part, called a pattern. The pattern is made slightly larger than the desired size of the final casting to account for shrinkage during cooling. This pattern is placed in a molding box, which is then half filled with a mixture of sand (crushed rock), clay and water. The sand is tightly packed around the pattern, and then the box is turned and the process is repeated with the top half of the pattern. The two mold halves are then separated and the pattern is removed. This pattern can then be used to generate additional molds, if necessary. A hole, called a sprue, is punched into the top of the mold to allow molten metal to be poured into the mold. Additional holes, known as risers, are also punched into the pattern to allow gas to escape. The sand casting process is often far less expensive than other techniques, and is often one of the fastest methods available. It does suffer from some disadvantages, however. First, it typically yields tolerances of 0.030 inches for the first foot, and then an additional 0.010 for each additional three inches. It also produces a product that requires further machining. At the very least, the casting must be separated from the risers and the sprue. Most applications also require additional finishing services, such as shot and hammer peening, grinding, forging or plating. These processes create a much finer surface, and are particularly important any time that the casting will be used as visible component.

The advantages of sand casting often outweigh its drawbacks. It produces less waste than a number of other machining processes, especially since unused material can simply be added to the next mold. It can achieve a wide range of shapes with a brief turnaround, especially when based on previously used molds or standard designs. It is also useful with many aluminum alloys, and can be effective with components weighing ounces or tons. It still plays an important role in the production of large metal forms, and can offer the advantages of low cost, quick results and ease of duplication to those goldsmiths who take the time to master it. Though sometimes thought of as coarse, sand casting can yield results that are as fine and true to detail as any other casting method.

### **3.2 SOLIDIFICATION PROCESS IN CASTING**

The casting process is essentially solidification of liquid metal in the mold cavity. Such a phase change from liquid to solid state involves the phenomena like changes in fluidity, volumetric shrinkage, segregation, evolving of gases absorbed and the size of grains which have profound influence on the quality of the final casting obtained. A proper understanding of solidification mechanism helps in avoiding major casting defects like shrinkage, porosity hot-tears, cracks distortions and poor mechanical properties.

- i. Alloys generally solidify as (a) solid solutions (b) eutectics or (c) combination of both, which are the most common. Information like liquidus (melting) temperature, solidification or freezing range, the different phases present at room temperature as well as at different temperatures for any particular alloy can be obtained from the phase diagram. Alloys with larger freezing range have lower fluidity depends upon the cooling rate.
- ii. During the cooling of a liquid alloy, on reaching liquidus temperature, solid particles or nuclei are first formed. They gradually grow in different directions based on the rate of heat loss, in tree-shaped dendrites, trapping the balance liquid in between their solid branches. The dendrites grow till they touch the adjoin

normally pursued to the grain boundaries. The size and type of grains formed depend upon the type of alloy, rate of heat extraction from liquid metal in the mold cavity and the geometry of the casting. As finer grains have superior mechanical properties like tensile strength, toughness and ductility, it is the attempt of every foundry to create conditions favorable to their formation and avoid coarse and columnar grains. The conditions that help in fine equiaxial grain formation are:

- a. Shorter freezing range-alloy,
  - b. Faster cooling of liquid metal as in metal molds/chills,
  - c. Larger surface area: volume ratio of casting having thin walls,
  - d. Higher pouring temperature.
- iii. During solidification from liquid to solid state, Aluminum alloy with long freezing range tend to develop casting defects like hot-tears and cracks. This happens during the stage of solidification when the solid dendrites while contracting are still not strong enough to overcome the hindrance offered by non-collapsible cores and mold. At this stage cracks start forming which could develop into serious casting defects later. Some of measures taken to avoid these include selection of an alloy with similar solidification range, change in design of casting to more a streamlined section and cooling time.
- iv. Dimensional changes, distortion and warpages in castings occurring during contraction of cast metal in the solid state to room temperature also depend upon the solidification characteristics of the alloy, the casting geometry and the temperature gradients in mold during cooling. They can be controlled by proper use of chills and changes in casting design.

Casting of AL-alloys is one of the most important features of Al technology for understanding the development of thermal stress and the prediction of residual



problems involving solid-liquid phase change. Furthermore, in a material undergoing phase change, there is volume change associated with difference in solid liquid densities of the material. If the density of solid phase in solidifying material is greater than that of liquid phase, this volume change is negative and is referred to as solidification shrinkage. During solidification, the density difference requires the melt to move towards the solid front; therefore a velocity field is induced in the melt. This velocity field produces several impacts on the solidifying material: changing the final shape, producing porosities, changing the solidified composition in alloys and consequently affecting the mechanical properties of material. Even if the castings were subjected to no constraints at all from the mould, it would certainly suffer from internally generated constraints as a result of uneven cooling. A well-known example of this effect is the mixed-section casting. If a failure occurs, it always happens in the thicker section. This may at first sight be surprising. The explanation of this behavior requires careful reasoning. First, the thin section solidifies and cools. Its contraction along its length is easily accommodated by the heavier section, which simply contracts under the compressive load since it is hot, and therefore plastic, if not actually still molten. Later, however, when the thin section has practically finished contracting, the heavier section starts to contract. It is unable to compress the thin section, which has now become rigid and strong. Thus, the heavy section goes into tension. Depending on its temperature it will stretch plastically, or hot tear, or cold crack.

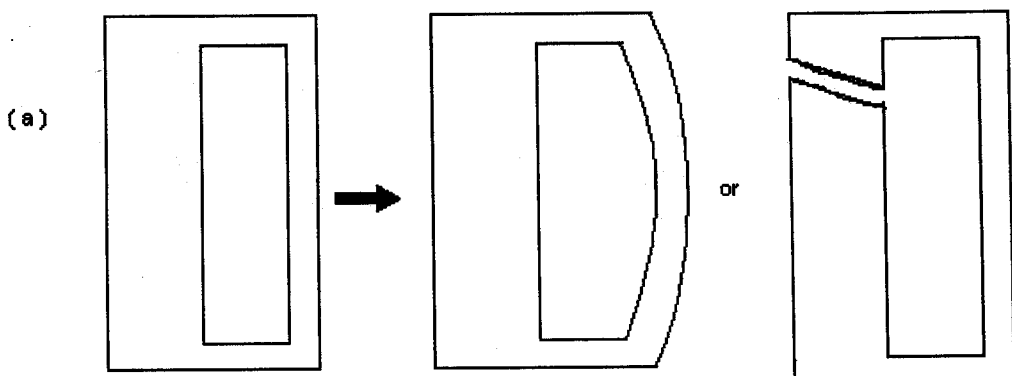


**FIGURE 3.1 (a) A THICK/THIN SECTION CASTING SHOWING TENSILE STRESS IN THE THICK SECTION**

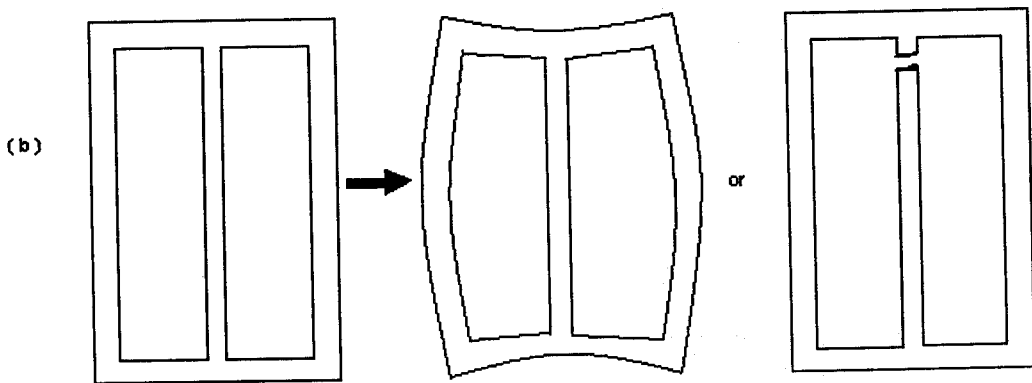


**FIGURE 3.1 (b) AN EVEN WALLED CASTING SHOWING INTERNAL TENSILE STRESSES**

The internal walls of the castings remain hot longest even though the casting may have been designed with even wall sections. This is, of course, simply the result of the internal sections being surrounded by other hot sections. The internal walls of the casting suffer tension at a late stage of cooling. This tension may be retained as a residual stress in the finished casting or lead to failure by tearing or cracking as shown in Figure 3.1 (a), (b). The same reasoning applies to the case of a single-component heavy-section casting such as an ingot, billet or slab, especially when these are cast in steel because of its poor thermal conductivity. The inner parts of the casting solidify and contract last, putting the internal parts of the casting into tension. Because of the low yield point of the hot metal, extensive plastic yielding occurs.

Premium quality aluminum castings are those with minimum guaranteed properties, either throughout the part or in particular locations. They can be made in sand and in metallic moulds. Proper placement of chills is essential. Further a strict control is exercised on the design of casting and on foundry practice. The aluminum alloys are large freezing range freeze with a region ahead of solidified a portion, in which solid crystals and liquid are present together, i.e. a mushy zone shown Figure 3.2.

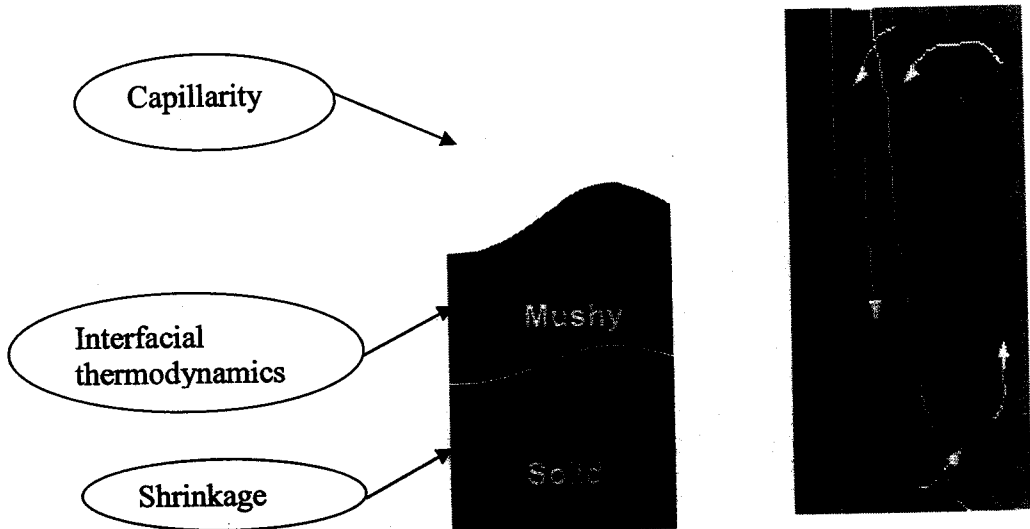


**FIGURE 3.2 PHYSICAL MECHANISMS IN SOLIDIFICATION**

### 3.2.1 Causes of solidification defects

- Density changes due to solidification.
- Gravitational effect.
- Thermal and physical properties of alloy.
- Residual force on phase change interface.
- Non – uniform heat extraction.
- Improper contact at metal/mold interface.

# *Chapter 4*

## *Casting Geometry*

## 4.1 INTRODUCTION

The casting geometry considered was 3(1/2) inch square bar surrounded on all sides by 3(1/4) inch of molded sand as shown in Figure 4.1. The casting was of sufficient length that heat transfer at the half-length plane was essentially two-dimensional, was cast in aluminum using dried molding sand.

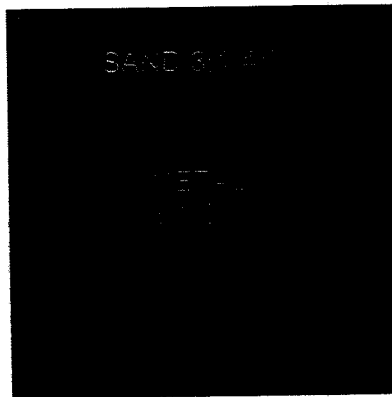


**FIGURE 4.1 CASTING GEOMETRY**

The casting was modeled assuming two-dimensional, symmetric heat flow at the half-length plane. Simulation of the solidification process was based on explicit finite difference approximations to the equations describing two-dimensional conduction heat transfer from the casting. The casting cross section was divided into a number of small control volumes using Cartesian grid system. Simulation output was in the form of grid node temperatures at specified nodes.

## 4.2 CASTING COMPOSITION

Aluminum alloys are the most widely used alloys. It is easily formed, machined, and cast. Alloys close to this composition have excellent fluidity, low shrinkage and high strength. The alloy is not heat-treatable. It enhances fluidity for thin walled or pressure tight castings and for the intricate shapes. It is used for automotive castings, motor housing, pump parts and domestic equipment. Pure

conductivity. In consequence it is widely used for foil and conductor cables, but alloying with other elements is necessary to provide the higher strengths needed for other applications.

**TABLE 4.1 TYPICAL PROPERTIES FOR ALUMINUM**

<b>PROPERTIES</b>	<b>VALUE</b>
Atomic Number	13
Atomic Weight (g/mol)	26.98
Valency	3
Crystal Structure	Face centered cubic
Melting Point (°C)	660.2
Boiling Point (°C)	2480
Mean Specific Heat (0-100°C) (cal/g.°C)	0.219
Thermal Conductivity (0-100°C) (cal/cms. °C)	0.57
Co-Efficient of Linear Expansion (0-100°C) ( $\times 10^{-6}/^{\circ}\text{C}$ )	23.5
Electrical Resistivity at 20°C ( $\mu\text{Ocm}$ )	2.69
Density ( $\text{g}/\text{cm}^3$ )	2.6898
Modulus of Elasticity (GPa)	68.3
Poissons Ratio	0.34

Premium quality aluminum castings are those with minimum guaranteed properties, either throughout the part or in particular locations. They can be made in sand and in metallic moulds. Proper placement of chills is essential. Further a strict control is exercised on the design of casting and on foundry practice. The properties of aluminum are shown in the table 4.1. The aluminum alloys are large freezing range freeze with a region ahead of solidified a portion, in which solid crystals and liquid are present together, i.e. a mushy zone.

Aluminum's range of properties can be found in an impressive array of commercially available alloys. The composition and logic of those alloys are regulated by an internationally agreed classifications system or nomenclature for wrought alloys and by v Strength depends on purity. 99.996 per cent pure aluminum has a tensile strength of about 49 megapascals (MPa), rising to 700

nature, Aluminum is an abundant element in the earth's crust. A key property is low density. Aluminum is only one-third the weight of steel. Aluminum and most of its alloys are highly resistant to most forms of corrosion. The metal's natural coating of aluminum oxide provides a highly effective barrier to the ravages of air, temperature, moisture and chemical attack. Aluminum is a superb conductor of electricity. This property allied with other intrinsic qualities has ensured the replacement of copper by aluminum in many situations. Aluminum is non-magnetic and non-combustible, properties invaluable in advanced industries such as electronics or in offshore structures. Aluminum is non-toxic and impervious, qualities that have established its use in the food and packaging industries since the earliest times. Other valuable properties include high reflectivity, heat barrier properties and heat conduction. The metal is malleable and easily worked by the common manufacturing and shaping processes.

### **4.3 EXPERIMENTAL RESULTS**

The experimental results are taken from American Foundry Service Transaction (AFS) journal named "Numerical Simulation of Casting Solidification" by R.D.Pehlke, M.J.Kirt, R.E.Marrone, and D.J.Cook.

#### **4.3.1 Introduction**

A 3-(1/2) inch square bar, sufficiently long so that heat transfer at the half-length plane was essentially two dimensional, was cast in aluminum silicon alloy using dried molding sand. The casting was a 3-(1/2) inch square bar surrounded on all three sides by 3-(1/4) inch of molded sand. Isochronal solidification profiles, cooling curves of specified location and temperature distribution along specified paths were obtained by monitoring the output of thermocouples placed at known cross sectional locations. Additional thermocouples measured the symmetry and two-dimensionality of the heat flow as the casting solidifies. Thermal properties of the materials involved, including the molding sand, were reasonably known as the functions of temperature.

### 4.3.2 Experimental Procedure

The castings were made using aluminum, butt-welded chromel-alumel thermocouple. Additional thermocouple located throughout the casting and in the mold. Measurements from these thermocouples indicate the assumptions of two dimensionality; symmetric heat flux at the half-length plane was valid. Handling of the emf output from the thermocouples was facilitated through use of a computer program, which converts emf to temperature, accounting for standardization and reference temperatures. The molds are hand rammed using 4% western bentonite, 2.5% water, and AFS mesh new jersey silica sand with nominal green compressive strength of 4.8 at a nominal green hardness of 75.

### 4.3.3 Results

Aluminum was poured at 2350 °F. Cooling curve at a number of locations, were obtained by monitoring the output of the thermocouple array as the casting cooled. The time, temperature data provide enough information to plot solidification profiles. Measurement from a thermocouple array in the sand was recorded.

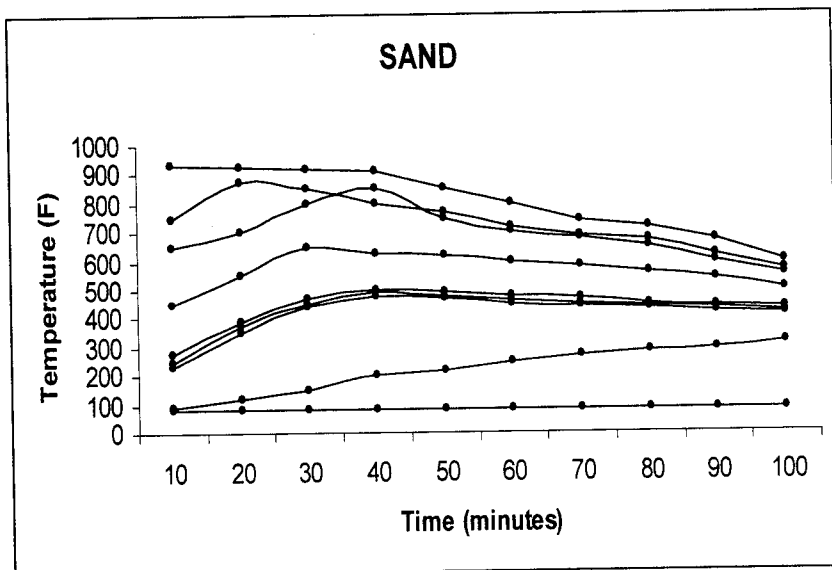
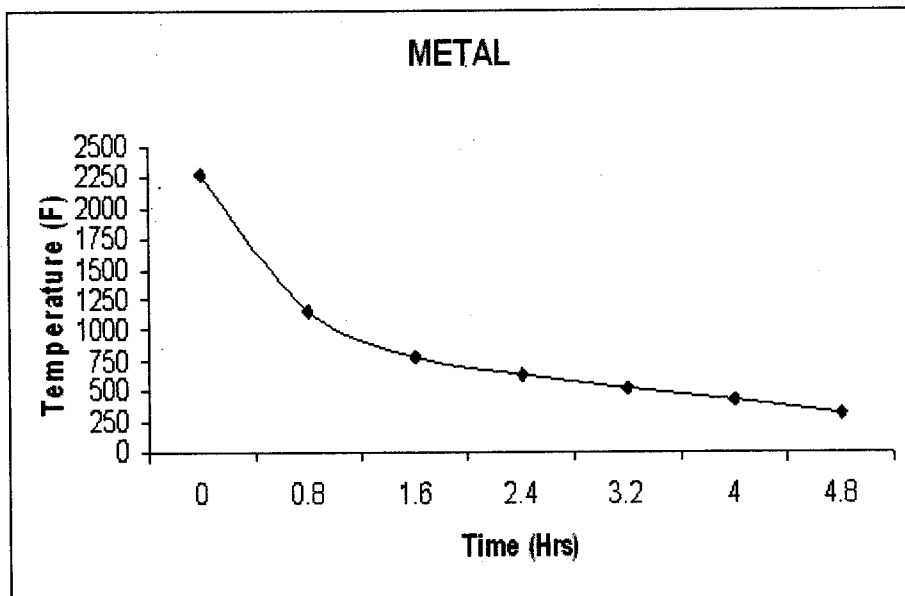


FIGURE 4.2 TEMPERATURE MEASUREMENTS IN SAND



The measurements from the thermocouple array in the sand are shown in the Figure 4.2. Initially the sand is at the ambient temperature. When the molten metal is poured into the mold, the temperature in the sand starts increasing, after certain period the temperature reduces gradually. The temperature at different nodes in the sand region varies more as compared to metal and interface temperature. The node near the interface region has the highest temperature and the value reduces gradually as the node considered is apart from the interface region.



**FIGURE 4.3 THERMOCOUPLE MEASUREMENTS OF COOLING CURVES IN EXPERIMENTAL CASTING OF ALUMINUM.**

In considering the solidification of metal, the temperature at different nodes gradually decreases as time increases. The molten metal, which is poured in to the mould, is initially at the temperature of 2350 °F. When the molten metal enters the mould the temperature starts reducing, as the surrounding temperature is 80 °F. As the molten metal enters the mould the temperature reduces to 2100 °F as shown in Figure 4.3.

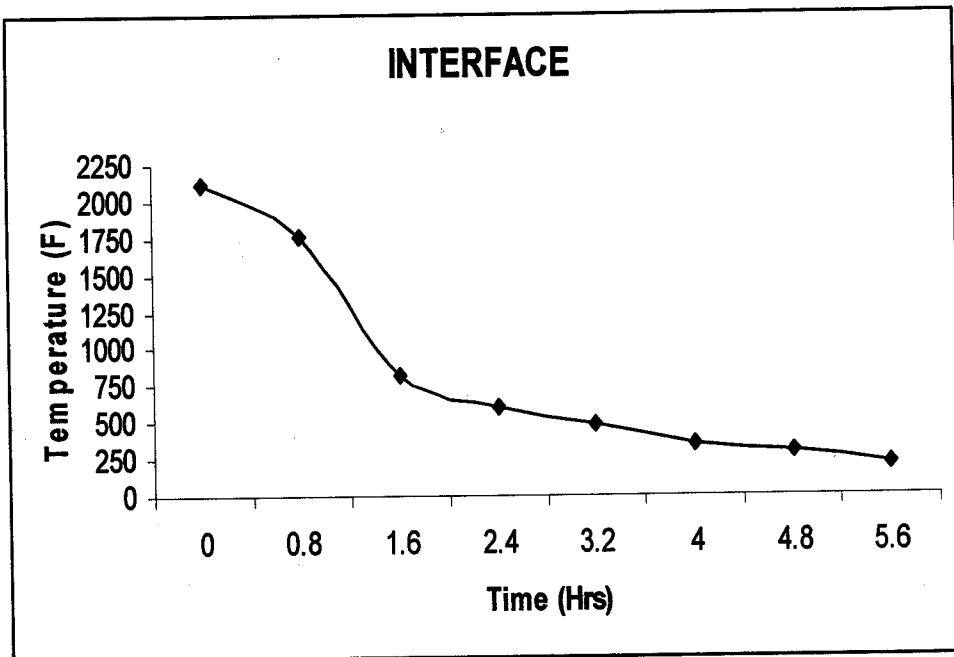


**FIGURE 4.4 THERMOCOUPLE MEASUREMENTS OF COOLING CURVES IN THE INTERFACE REGION.**

The temperatures at the interface region are similar to cast region. The interface temperature reaches to 1900 °F when the molten metal is poured into the mould. At 5.5 hrs the temperature of the interface region reduces to 200 °F as shown in Figure 4.4.

# *Chapter 5*

*Development of Node*

## 5.1 INTRODUCTION

The explicit difference approximation method divides space and time into discrete uniform subintervals and replaces time and space derivatives by finite difference approximations, permitting one to easily compute values of the function at a time  $\Delta t$  after the initial time. These values are then used to compute a second set of values and the process is repeated.

## 5.2 GENERAL NODE

Consider a general node and its associated control volume, if  $\frac{dT}{dt}$  is approximated

by  $\left[ \frac{(U'_{i,j} - U_{i,j})}{\Delta t} \right]$

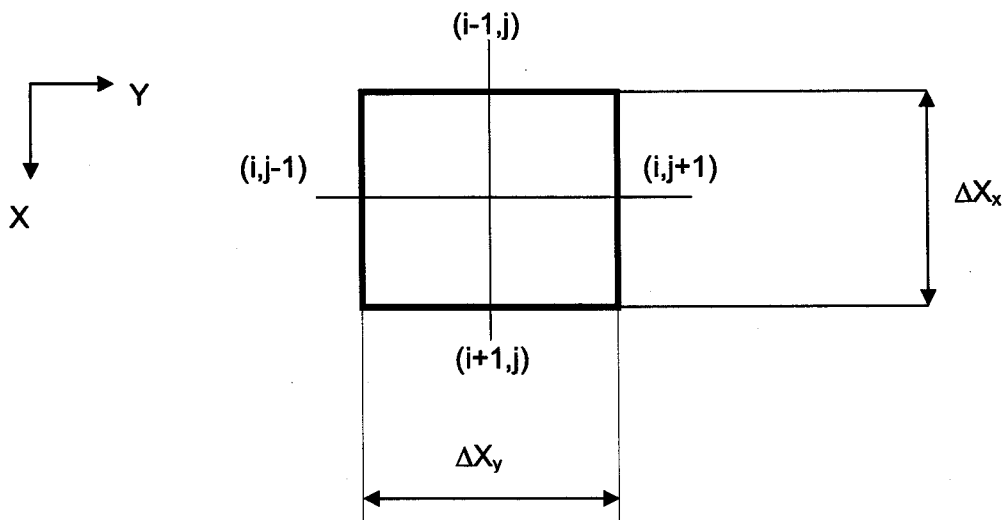


**FIGURE 5.1 GENERAL NODE AND ITS ASSOCIATED CONTROL VOLUME**

First law of thermodynamics applied to the control volume shown in Figure 5.1 is stated symbolically as

$$PCp\Delta X_x\Delta Y_y \left[ \frac{(U'_{i,j} - U_{i,j})}{\Delta t} \right] = (Q_{(i-1,j)} + Q_{(i+1,j)} + Q_{(i,j+1)} + Q_{(i,j-1)}) \text{-----}(5.1)$$

If heat is assumed to flow into the control volume from the surrounding nodes,

$$Q_{(i+1,j)} = k\Delta X_x \left[ \frac{(U_{(i+1,j)} - U_{(i,j)})}{\Delta X_y} \right]$$

The subscript as refers to any of the surrounding nodes. If  $\Delta X_x = \Delta Y_y$ , after making the substitutions for  $Q_{SS}$  as (i, j) in terms of  $U_{SS}$  to  $U_{i,j}$ . The equation 1 reduces into

$$U'_{i,j} = \left[ \frac{k\Delta t}{PCp\Delta X^2} \right] (U_{(i-1,j)} + U_{(i+1,j)} + U_{(i,j+1)} + U_{(i,j-1)} - 4 U_{(i,j)}) + U_{(i,j)} \text{-----}(5.2)$$

Equation 5.2, expresses the future temperature of node (i,j) in terms of the present temperature of node (i,j) and the present temperature of surrounding node, all of which are known. Similar equations can be developed for the specialized nodes.

### 5.3 CORNER NODE

Consider the node on the diagonal symmetry plane for the sand-metal interface, i.e. the corner of the casting.

For this node, shown in Figure 5.2.

$$\text{Volume of the sand} = (3/8) \Delta X^2$$

$$\text{Volume of the metal} = (1/8) \Delta X^2$$

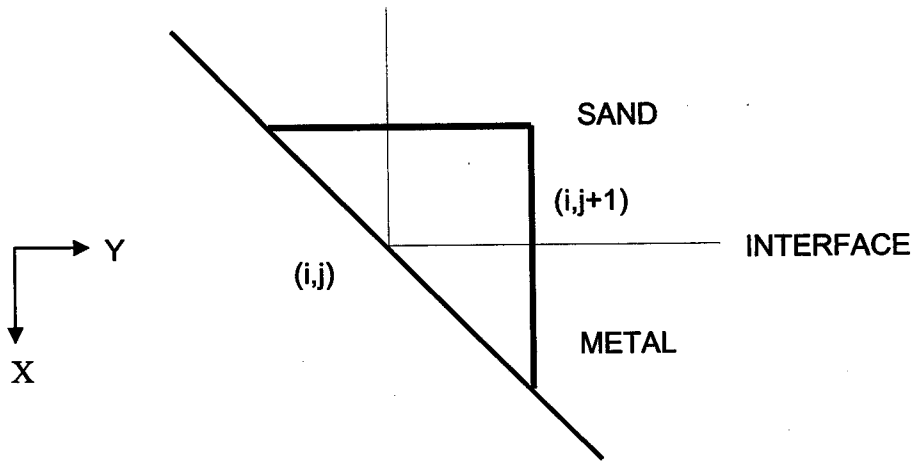


**FIGURE 5.2 NODE AND CONTROL VOLUME ASSOCIATED WITH THE CORNER OF THE CASTING.**

$$\text{Net rate of thermal energy increase in sand} = (3/8) \Delta X^2 P_S C_{PS} \left[ \frac{(U'_{i,j} - U_{i,j})}{\Delta t} \right]$$

$$\text{Net rate of thermal energy increase in metal} = (1/8) \Delta X^2 P_M C_{PM} \left[ \frac{(U'_{i,j} - U_{i,j})}{\Delta t} \right]$$

Hence, Net rate of thermal energy increase in control volume is

$$\{[(3/8) P_S C_{PS}] + [(1/8) P_M C_{PM}]\} \Delta X^2 \left[ \frac{(U'_{i,j} - U_{i,j})}{\Delta t} \right]$$

$$\text{Heat influx from node } (i-1, j) = K_S \Delta X_X (1/2) \left[ \frac{U_{(i,j+1)} - U_{i,j}}{\Delta X_Y} \right] +$$

$$K_M \Delta X_X (1/2) \left[ \frac{U_{(i,j+1)} - U_{i,j}}{\Delta X_Y} \right]$$



Conservation of thermal energy yields,

$$U'_{ij} = \left[ \frac{4\Delta t}{(3P_S C_{PS} + P_M C_{PM})\Delta X^2} \right] [\{2 K_S U_{(i-1,j)}\} + \{ (K_S + K_M) U_{(i,j+1)} \} - \{ (K_M + 3 K_S) U_{ij} \} + U_{ij}] \text{ ----- (5.3)}$$

Equations for the future temperature of the other specialized nodes (sand-metal interface nodes on symmetry plane) are developed as above procedure. Thermal properties of the materials are assumed to be those corresponding to the present temperature of node (i,j).

## 5.4 STABILITY OF THE APPROXIMATIONS

Equation 5.2 can be rewritten as

$$U'_{ij} = \{ M(U_{(i-1,j)} + U_{(i+1,j)} + U_{(i,j+1)} + U_{(i,j-1)}) + (1-4M) U_{(i,j)} \}$$

Here, 
$$M = \left[ \frac{k\Delta t}{PC_p\Delta X^2} \right]$$

The influence on the future temperature at node (i,j) is the sum of the surrounding node temperatures and the present temperature of node (i,j) as the function of M. At  $M = (1/4)$  the future temperature of node (i,j) is independent of the present temperature of node (i,j). for M Greater than (1/4), the present temperature of node (i,j) has a negative influence on the future temperature of node (i,j). Hence, stability or physical realism requires

$$0 < M < (1/4), \text{ or } \Delta t < [(PC_p\Delta X^2) / 4k].$$

Thus for any arbitrary grid size,  $\Delta X$ , There is an upper limit on the size of the time increment which can be obtained from the specialized node equations.

## 5.5 INITIAL TEMPERATURE DISTRIBUTION

Initially (at time is zero) the sand is assumed to be at ambient temperature. The initial metal temperature is assumed to be the temperature of the metal as it enters the

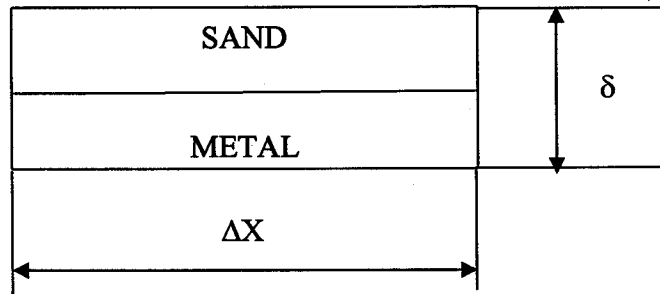


**FIGURE 5.3 CONTROL VOLUME CONSIDERED WHEN CALCULATING THE INITIAL SAND-METAL INTERFACE TEMPERATURE.**

The thermal energy initially contained in this system is

$$\left\{ (1/2) \delta \Delta X ( P_M C_{PM} T_{Om} + P_S C_{PS} T_{Os} ) \right\}$$

Allow to come adiabatically to equilibrium. The adiabatic assumption is reasonable since as  $\delta$  tends to zero. What ever happens to the system is assumed to happen instantly. Also, by definition of this initial condition, no heat flux has yet been established, hence no heat is transferred to or from the system.

There are three possible final states for the system depending on the relative values of  $P_M, C_{PM}, P_S, C_{PS}, T_{Os}, T_{Om}$ .

### 5.5.1 None Of The Metal Solidifies.

Equating the thermal energy in the system initially to that in the system, as equilibrium yields,

$$\left\{ (1/2) \delta \Delta X ( P_M C_{PM} T_{Om} + P_S C_{PS} T_{Os} ) \right\} = \left\{ (1/2) \delta \Delta X ( P_M C_{PM} + P_S C_{PS} ) T_1 \right\}$$

Where  $T_1$  is the initial interface temperature.



$$T_I = \left[ \frac{(P_M C_{PM} T_{Om} + P_S C_{PS} T_{Os})}{(P_M C_{PM} + P_S C_{PS})} \right]$$

The properties of the sand and metal in the numerator are at  $T_{Om}$  and  $T_{Os}$ , initially assuming a value for  $T_I$ , take the sand and metal properties for the denominator at this  $T_I$ , and calculate a new  $T_I$ , then continue the iteration. This converges rapidly (three or four iterations) to a single value of  $T_I$ , this same iterative process must also be used for cases 5.5.2 and 5.5.3.

### 5.5.2 All Of The Metal Solidifies.

The thermal energy released when the metal solidifies is  $\{(1/2) \delta \Delta X\} P_M \{\Delta H_F\}$

Conservation of energy yields

$$\{(1/2) \delta \Delta X (P_M C_{PM} T_{Om} + P_S C_{PS} T_{Os})\} + \{(1/2) \delta \Delta X\} P_M \{\Delta H_F\} =$$

$$\{(1/2) \delta \Delta X (P_M C_{PM} + P_S C_{PS}) T_I\}$$

Hence,

$$T_I = \left[ \frac{(P_M C_{PM} T_{Om} + P_S C_{PS} T_{Os} + P_M \Delta H_F)}{(P_M C_{PM} + P_S C_{PS})} \right]$$

### 5.5.3 The Metal Partially Solidifies

If the liquidus and solidus of the binary system are approximated by straight lines, the fraction of liquid solidifies as a function of temperature, can be expressed as

$$FS = \text{Fraction Solidified} = \left[ \frac{1}{[(1 - B) + [AB / (T_{st} - T_I)]]} \right]$$

Where,

$A = (T_{st} - T_f)$  [Temperature at which solidification begins minus temperature at which

$B = \{(\tan\theta) (\cot\phi)\}$  [ $\theta$  and  $\phi$  are angles between the liquidus and solidus and an isotherm].

For a pure metal, the liquidus and solidus are parallel (same line) and the above expression reduces to

$$FS = \left[ \frac{(T_{st} - T_l)}{(T_{st} - T_f)} \right]$$

Equating thermal energy in the system initially to that in the system at equilibrium yields

$$\{(1/2) \delta \Delta X) ( P_M C_{PM} T_{Om} + P_S C_{PS} T_{Os} )\} + \left[ \frac{(T_{st} - T_l)}{(T_{st} - T_f)} \right] [ P_M \{ \Delta H_f \} ] [(1/2) \delta \Delta X] = \{(1/2) \delta \Delta X) ( P_M C_{PM} + P_S C_{PS} ) T_l \}$$

Hence,

$$T_l = \left[ \frac{\{ ( P_M C_{PM} T_{Om} + P_S C_{PS} T_{Os} ) + [(T_{st} P_M \Delta H_f) / (T_m - T_f)] \}}{( P_M C_{PM} + P_S C_{PS} ) + [P_M \Delta H_f / (T_m - T_f)]} \right]$$

The initial temperature of every node is specified. Using these equations, the temperature of each node at time ( $\Delta t$ ) can be calculated. When all the node temperature at time ( $\Delta t$ ) have been determined, temperatures at time ( $\Delta t$ ) become the present temperature node temperature at time ( $2\Delta t$ ) can be calculated. Similarly node temperature can be calculated to any time ( $n \Delta t$ ), when  $n$  is equal to 1, 2, 3 ...

# *Chapter 6*

*Computational Method*

## 6.1 INTRODUCTION TO ANSYS 8.1

The Ansys 8.1 provide the highest quality engineering tools to help with all of design and analysis needs. Ansys is the original (and commonly used) name for ansys mechanical or ansys multiphysics, general-purpose finite element analysis (FEA) computer aided engineering (CAE) software tools, but is perhaps best known for ansys mechanical & ansys multiphysics. Ansys mechanical and ansys multiphysics are self contained analysis tools incorporating pre-processing (geometry creation, meshing), solver and post processing modules in a unified graphical user interface. The software is used to analyze a broad range of applications. Ansys mechanical incorporates both structural and material non-linearities. Ansys multiphysics includes solvers for thermal, structural, cfd, electromagnetics, acoustics and can couple these separate physics together in order to address multi-disciplinary applications. Ansys software is also used in civil engineering, electrical engineering, physics and chemistry.

## 6.2 ANSYS LIMITS

The ansys 8.1 limits are listed in table 6.1.

**TABLE 6.1 ANSYS LIMITS**

<i>ANSYS ED FEA Limits</i>	
Maximum DOF	2,000 (14,000 for FLOTRAN)
Maximum Node Number	1,000 (2,000 for FLOTRAN)
Maximum Element Number	500 (2,000 for FLOTRAN)
Maximum Master DOF Number	50
<i>ANSYS ED Solid Modeling Limits</i>	
Maximum Key point Number	100
Maximum Line Number	100
Maximum Area Number	50
Maximum Volume Number	10

## **6.3 APPROACH AND ASSUMPTIONS**

Half symmetry is used to reduce the size of the model. The lower half is the portion you will model. The mold material (sand) has constant material properties. The casting (aluminum) has temperature-dependent thermal conductivity and specific heat; both are input in a table of values versus temperature. Radiation effects are ignored. Solution control is used to establish several nonlinear options, including automatic time stepping. Automatic time stepping determines the proper time step increments needed to converge the phase change nonlinearity. This means that smaller time step sizes will be used during the transition from molten metal to solid state.

## **6.4 SUMMARY OF STEPS**

1. The casting Geometry is given as input
2. Reading the geometry of the casting.
3. Defining the material properties.
4. Plotting the material properties vs. temperature graph.
5. Defining the element type.
6. Meshing the model.
7. Applying convection loads on the exposed boundary lines.
8. Defining analysis type.
9. Examining solution control.
10. Specifying initial conditions for the transient.
11. Setting time, time step size, and related parameters.
12. Setting output controls.
13. Solving the conditions.
14. Entering the time-history postprocessor and defining variables.
15. Plotting temperature vs. time.
16. Setting up to animate the results.
17. Animating the results.
18. Exiting the ANSYS program.

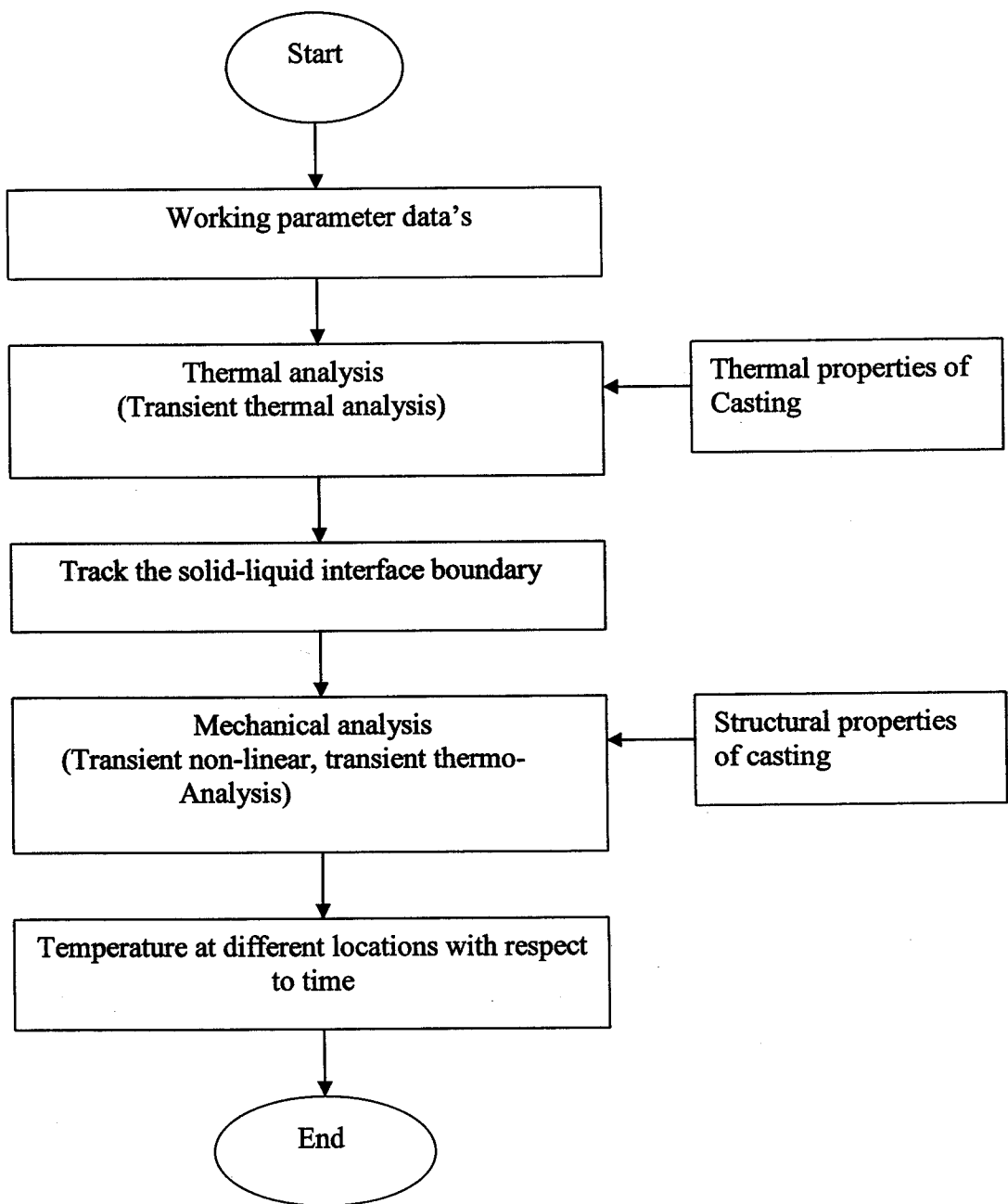


**FIGURE 6.1 SCHEMATIC DIAGRAM FOR ANALYSIS OF CASTING.**

## 6.5 PREPARATION FOR THERMAL ANALYSIS

### 6.5.1 Setting the Preferences.

Set the preference for Graphical unit interface as thermal.

### 6.5.2 Reading the Geometry of the Casting.

This step indicates the geometry input. Initially the key points are generated. Since here FPS system is considered the following key point values are  $(0,0)$ ,  $(0.4167,0)$ ,  $(0.416,0.1458)$ ,  $(0.4167,0.4167)$ ,  $(0,0.4167)$ ,  $(0.270,0.146)$ . These key points are connected through straight lines. Then areas are created as indicated in the diagram shown below in which A1 is sand area and A2 is metal area. The areas A1 and A2 are glued as shown in Figure 6.2.

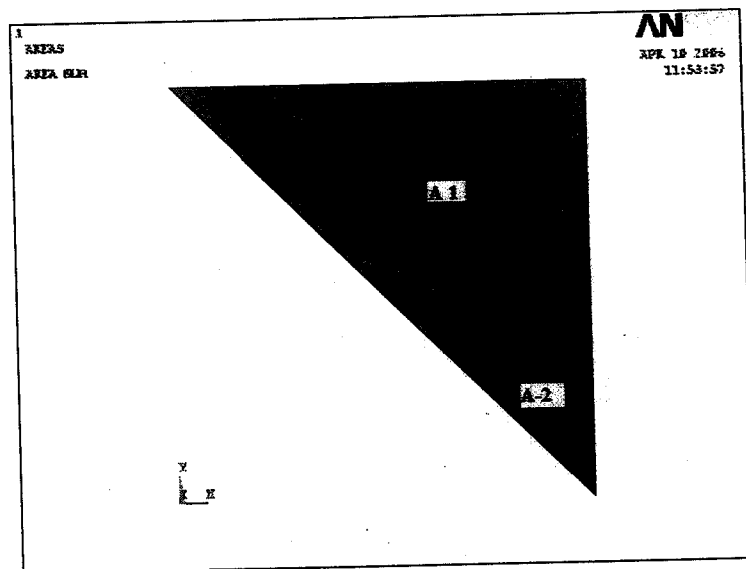


**FIGURE 6.2 GEOMETRY INPUT**

### 6.5.3 Defining Material Properties.

Here material properties are defined. Considering material number 1 as sand and material number 2 as Aluminum. The various material properties include thermal conductivity, specific heat, and density as shown in tables and figures with respect to the temperature. The density of aluminum is greater than sand.

**TABLE 6.2 DENSITY OF THE MATERIALS**

Density	(lb/ ft <sup>3</sup> )
Aluminum	169
Sand	102

**TABLE 6.3 SPECIFIC HEAT FOR SAND**

Temperature { °F }	Specific heat (C) { Btu/(lb-°F) }
200	0.19
400	0.22
800	0.25
1200	0.27
1600	0.28
2000	0.29

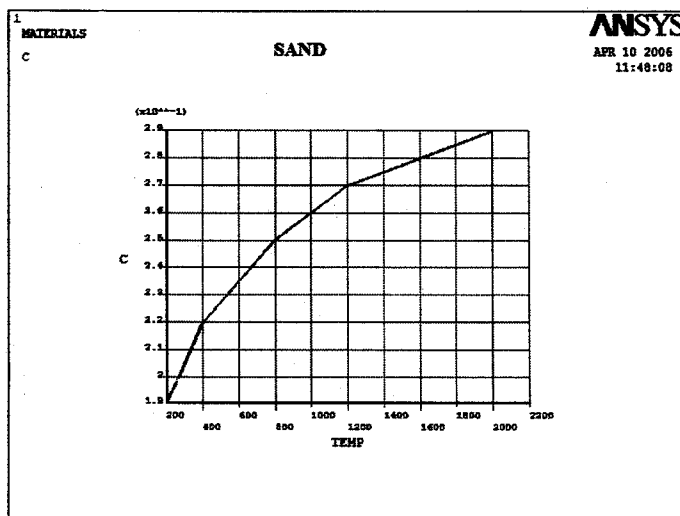


**FIGURE 6.3 SPECIFIC HEAT VS TEMPERATURE FOR SAND**



**TABLE 6.4 THERMAL CONDUCTIVITY FOR SAND**

Temperature {°F}	Conductivity (KXX) for sand {Btu/(hr-ft-°F)}
200	0.55
400	0.5
800	0.4
1200	0.5
1600	0.6
2000	0.8

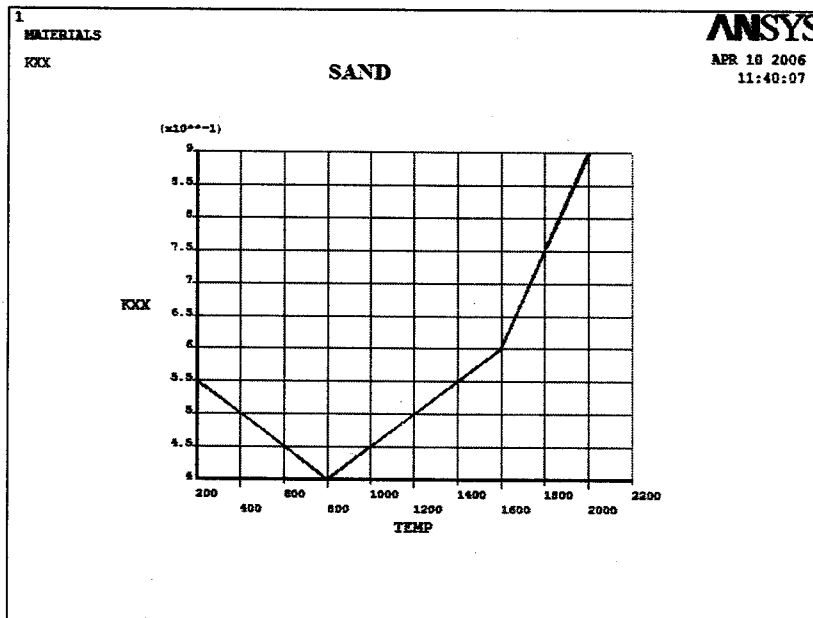


**FIGURE 6.4 THERMAL CONDUCTIVITY VS TEMPERATURE FOR SAND**

The various properties of aluminum at different temperatures are tabulated and plotted in graphical format. The units are in FPS system. The temperature is indicated in Farenheit, thermal conductivity in {Btu/(hr-ft-°F)} and specific heat in {Btu/(lb °F)}

**TABLE 6.5 THERMAL CONDUCTIVITY FOR ALUMINUM**

Temperature {°F}	Conductivity (KXX) for Aluminum {Btu/(hr-ft-°F)}
200	140
400	135
800	130
1200	110
1600	80
2000	60

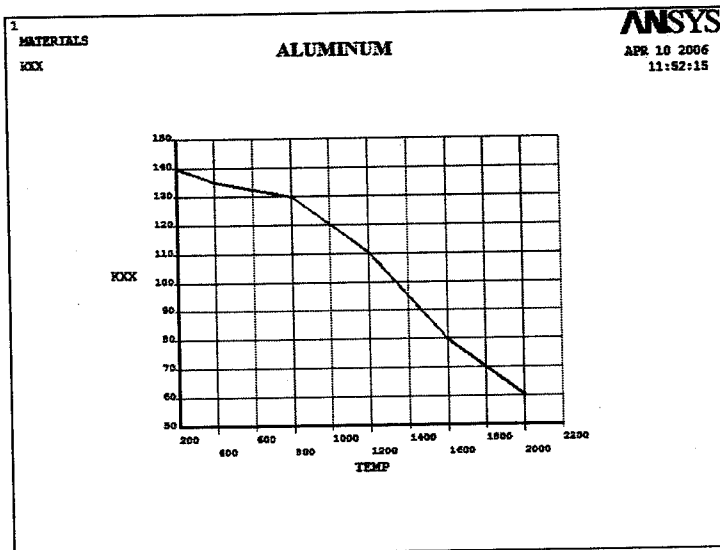


**FIGURE 6.5 THERMAL CONDUCTIVITY VS TEMPERATURE FOR ALUMINUM**

**TABLE 6.6 SPECIFIC HEAT FOR ALUMINUM**

Temperature {°F}	Specific heat (C) for Aluminum {Btu/(lb-°F)}
200	0.22
400	0.23
800	0.26
1200	0.28
1600	0.30

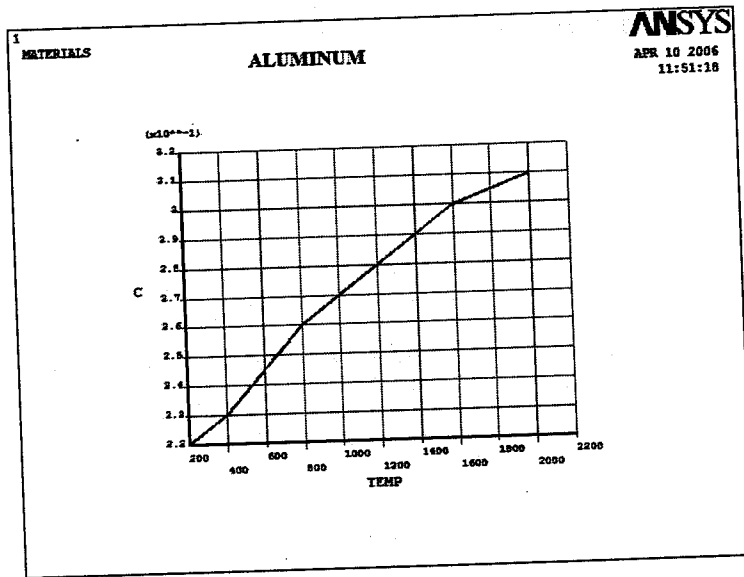


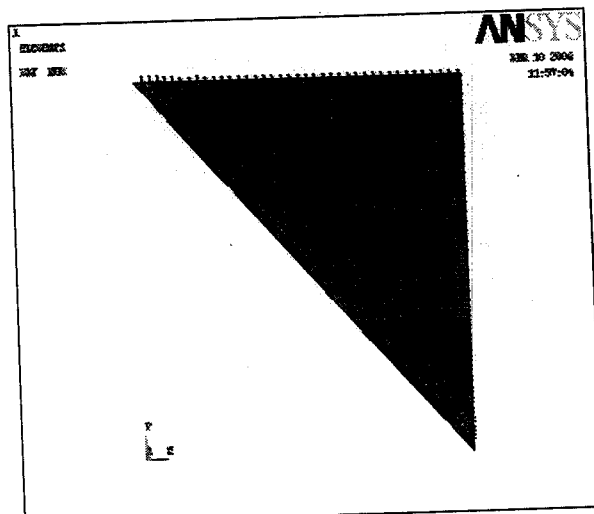
**FIGURE 6.6 SPECIFIC HEAT VS TEMPERATURE FOR ALUMINUM**

#### 6.5.4 Defining the Element Type.

The type of element selected is thermal solid – quad 4node 55.

#### 6.5.5 Meshing the Model.

The model is meshed separately for areal and area2. applying smart size, fine course number as 2, the areas are meshed. The elements of material 1 form the sand mold. The elements of material 2 form the aluminum casting. The elements are plotted showing materials in different colors without displaying the associate material numbers as shown in Figure 6.7.



### 6.5.6 Applying Convection Loads On The Exposed Boundary Lines.

Apply the convection to the lines of the solid model. Loads applied to solid modeling entities are automatically transferred to the finite element model during solution. Since, here half symmetry geometry is considered; the convection load is applied on the top line of the geometry, which is exposed to air as shown in Figure 6.8.

**TABLE 6.7 LOADS APPLIED**

Convection Properties	
Film coefficient	4 Btu/(hr-ft <sup>2</sup> -°F)
Ambient temperature	80 °F

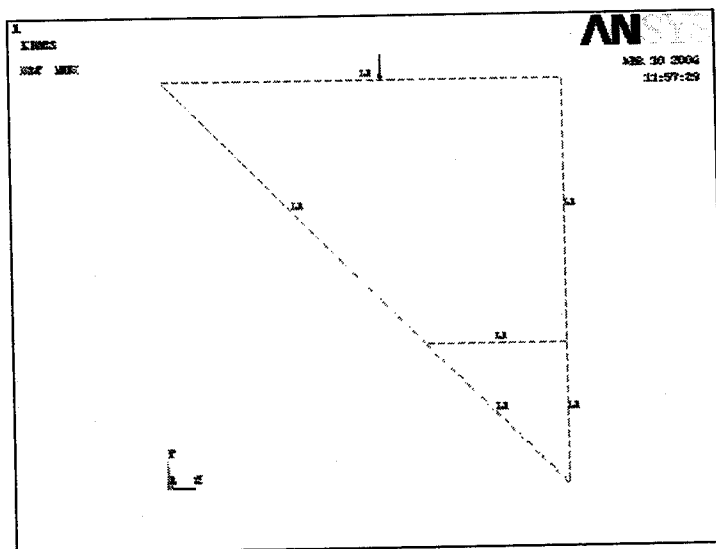


**FIGURE 6.8 CONVECTION LOAD ON TOP OF GEOMETRY**

### 6.5.7 Defining the Analysis Type.

### 6.5.8 Specifying Initial Conditions for The Transient.

The mold is initially at an ambient temperature of 80°F and the molten metal is at 2350°F. First selecting the casting area, then the nodes within that area and apply the initial molten temperature to those nodes. Next, invert the selected set of nodes and apply the ambient temperature to the mold nodes.

**TABLE 6.8 INITIAL CONDITIONS**

Initial Conditions	
Temperature of aluminum	2350 °F
Temperature of sand	80 °F

### 6.5.9 Setting the Time, Time Step Size, and Related Parameters.

The Stepped boundary conditions simulate the sudden contact of molten metal at 2350 °F with the mold at ambient temperature. The program will choose automatic time stepping that will enable the time step size to be modified depending on the severity of nonlinearities in the system (for example, it will take smaller time steps while going through the phase change). The maximum and minimum time step sizes represent the limits for this automated procedure. Time at the end of load step is assumed as 5.5-hrs. The-time step size is 0.01 and stepped boundary condition is considered. The maximum and minimum time step sizes are considered as 0.25 and 0.001 hrs. Automatic time step leads to improper results.

### 6.5.10 Setting the Output Controls.

The output controls are allowed to check for every subset.

### 6.5.11 Solving the conditions.

While ANSYS is solving the analysis, the Graphical Solution Tracking (GST) monitor plots the "Absolute Convergence Norm" as a function of the "Cumulative Iteration Number." The solution is assumed to have converged for

the end of load step is 5.5 hrs; the absolute convergence norm value is fluctuating with respect to the cumulative iteration number. After reaching around 85 iterations the absolute convergence norm value gets decreased as shown in Figure 6.9.

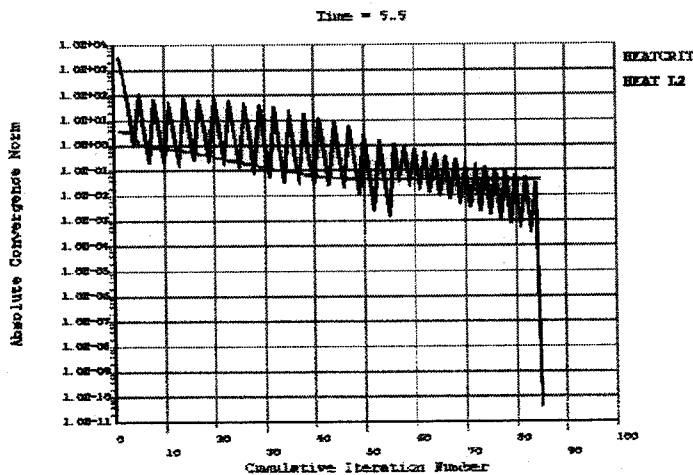


**FIGURE 6.9 ITERATION**

#### **6.5.12 Entering the Time-History Postprocessor and Define Variables.**

The time-history postprocessor option is used to look the variation of temperature with respect to time at one point on the casting (on the symmetry plane). By using a variable to identify the node at the center point, the analysis will be more flexible in that the center node will always be used even if the mesh, and therefore node numbers, changes. The variables are the nodes on metal or sand or interface.

#### **6.5.13 Plotting Temperature Vs Time.**

The plotted results between temperature and time are used to find the solidification region. Here the graph is drawn separately for metal, interface region and sand at different nodal regions. The initial temperature of the molten metal is considered as 2350 °F and sand is 80 °f. There is not much difference in variation of temperature with respect to time for metal and interface positions.

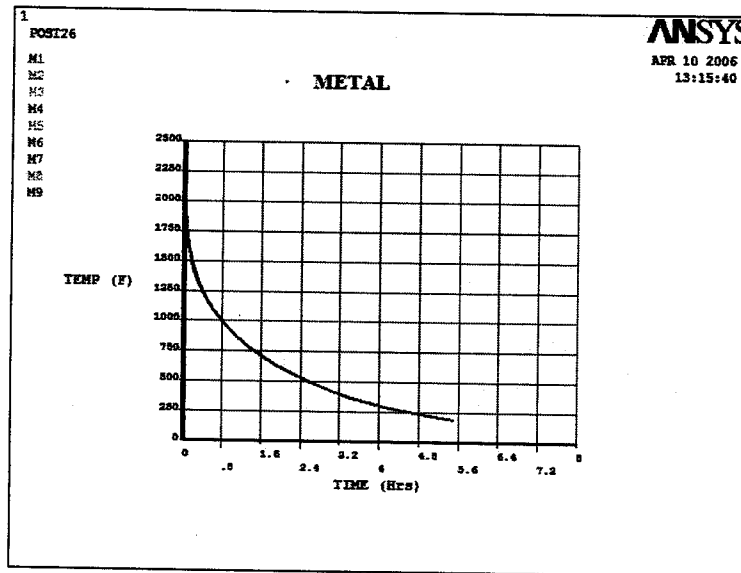


**FIGURE 6.10 TEMPERATURE VS TIME FOR METAL**

In considering the solidification of metal, the temperature at different nodes gradually decreases as time increases. The molten metal which is poured in to the mould is initially at the temperature of 2350 °F as shown in Figure 6.10. The temperatures at different nodes M1,M2,M3,M4,M5,M6,M7,M8,M9 are plotted with respect to time. When the molten metal enters the mould the temperature starts reducing, as the surrounding temperature is 80 °F. As the molten metal enters the mould the temperature reduces to 2100 °F. At 0.8 hrs the temperature decreases to 1000°F.the temperature reduces gradually after 1.6, 2.4, 3.2, 4, 4.8 hrs as 700,550,400,300and 250 °F respectively. The temperature after 5.5hrs decreases to 200 °F.

The temperatures at the interface region are similar to cast region as shown in Figure 6.11. The temperature at different nodal points I-1,I-2,I-3,I-4 are plotted with respect to time. The interface temperature reaches to 1900 °F when the molten metal is poured into the mould. The temperature further reduces to 1000,700,500,400,300,250 °F when the time increases to 0.8, 1.6, 2.4, 3.2,4, and 4.8 hrs respectively. At 5.5 hrs the temperature of the interface region reduces to 200 °F.

The temperature at different nodes in the sand region varies more as compared to metal and interface temperature as shown in Figure 6.12. The

near the interface region has the highest temperature and the value reduces gradually as the node considered is apart from the interface region.

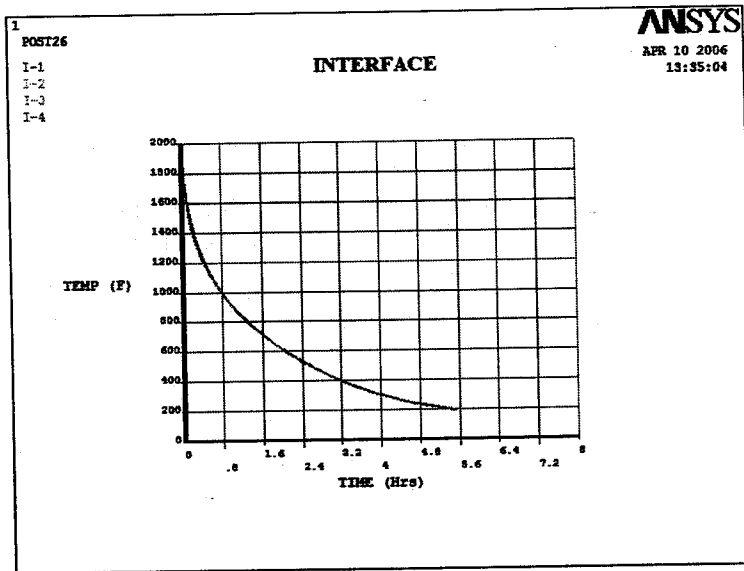


**FIGURE 6.11 TEMPERATURE VS TIME FOR INTERFACE REGION**

The node S1 is near the interface region, which has the initial temperature as 1000 °F ,and further increases to 1400 °F and starts stable after 2 hrs reaching 550 °F.

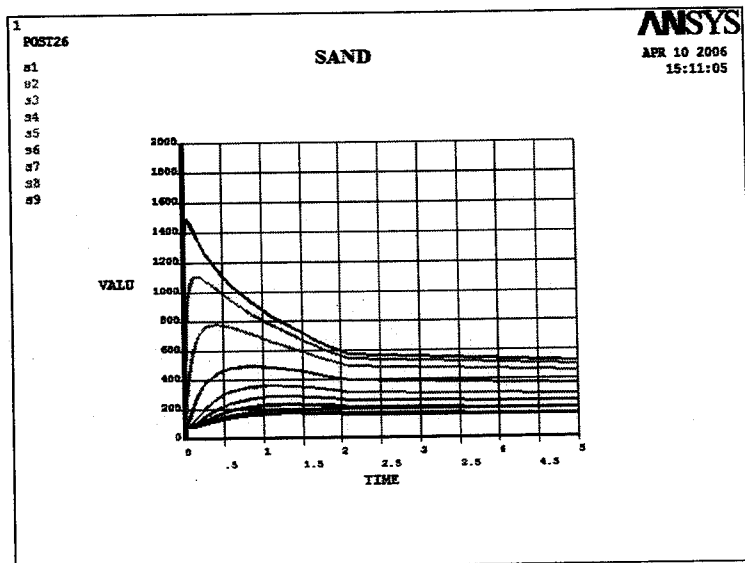


**FIGURE 6.12 TEMPERATURE VS TIME FOR SAND**



Generally the temperature in sand region increases and attains the stable condition and decreases slowly. The nodal points S2, S3, S4, S5, S6, S7, S8, S9 attains the temperature as mentioned above and reduces slowly.

#### 6.5.14 Animating the Results.

To better visualization of the solidification process, there is a necessity for animating the results. To capture the animation sequence in terminal segment memory, it is necessary to reduce the size of the Graphics Window or you will run out of terminal memory. The number of animation frames should be given. Temperatures at various locations can be found at different time intervals as shown in Figures 6.13, 6.14, 6.15, and 6.16. The following figure indicates the conditions at different locations. The regions are indicated in different colors that represent the temperatures at particular time after which the molten metal is poured into the mould.

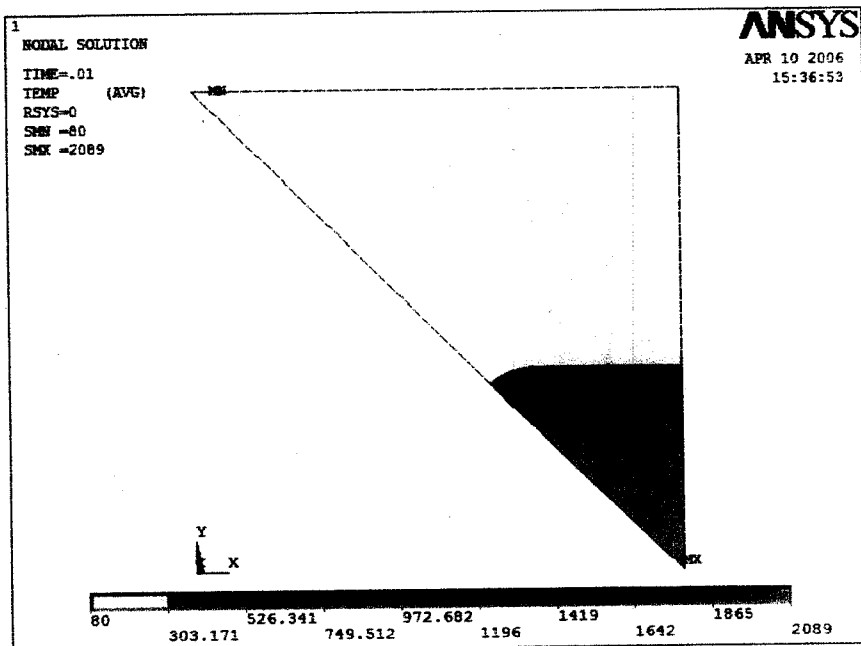


**FIGURE 6.13 TEMPERATURE DISTRIBUTION AT 0.01 HRS**

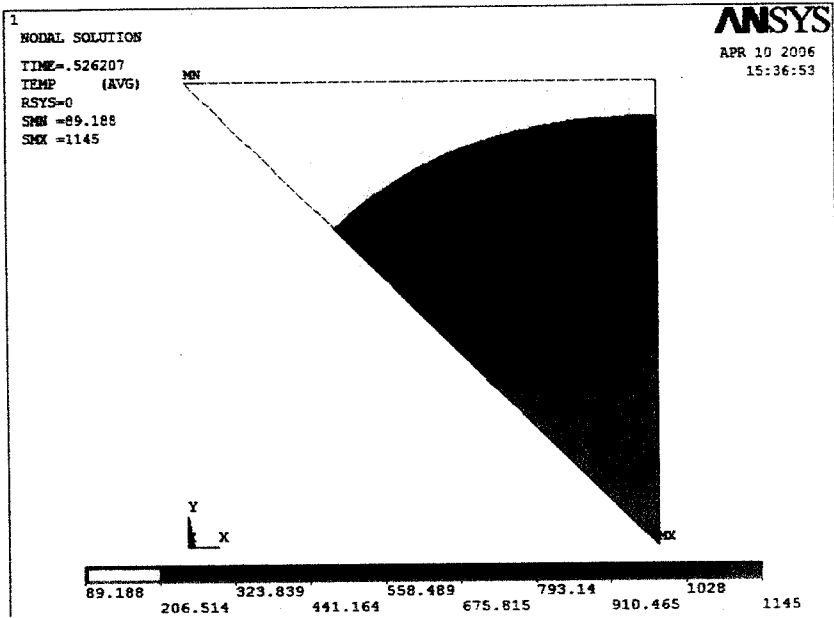


**FIGURE 6.14 TEMPERATURE DISTRIBUTION AT 0.52 HRS**

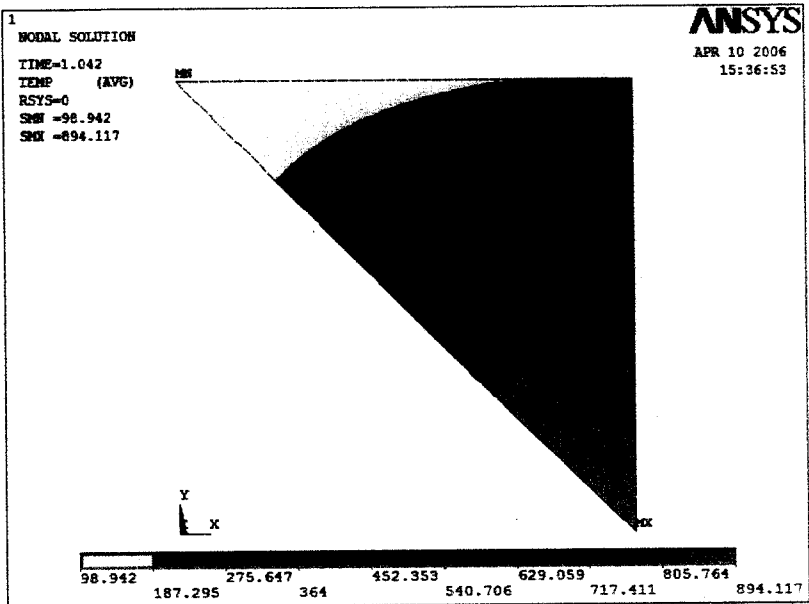


**FIGURE 6.15 TEMPERATURE DISTRIBUTION AT 1.04 HRS**

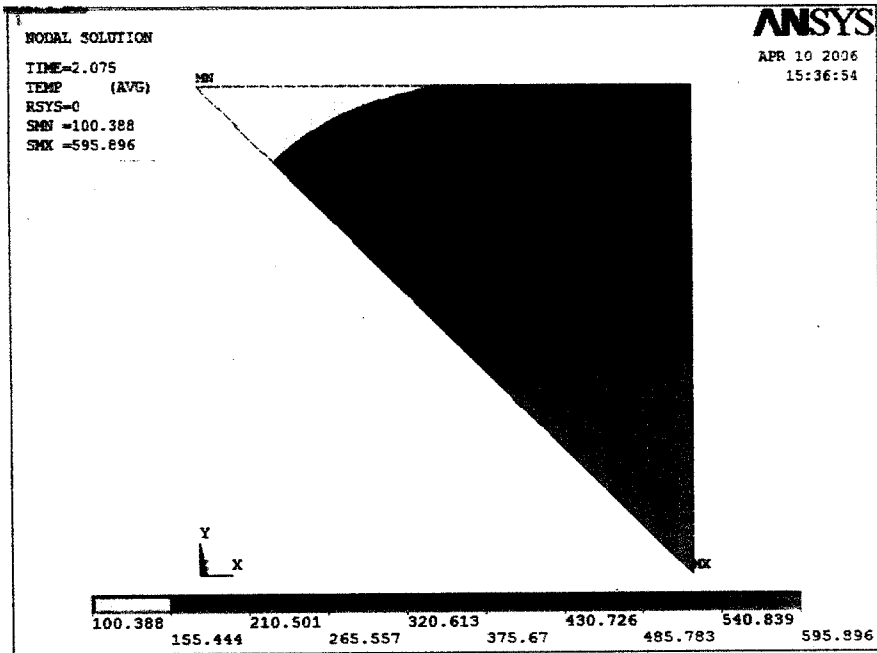


**FIGURE 6.16 TEMPERATURE DISTRIBUTION AT 2.075 HRS**

The animation will clearly explain the solidification of the casting geometry with respect to time. The results obtain can be used to optimize the process by suggesting various external aspects kept at various locations around the casting geometry.

# *Chapter 7*

*Algorithm and Flowchart  
for Thermal Analysis*

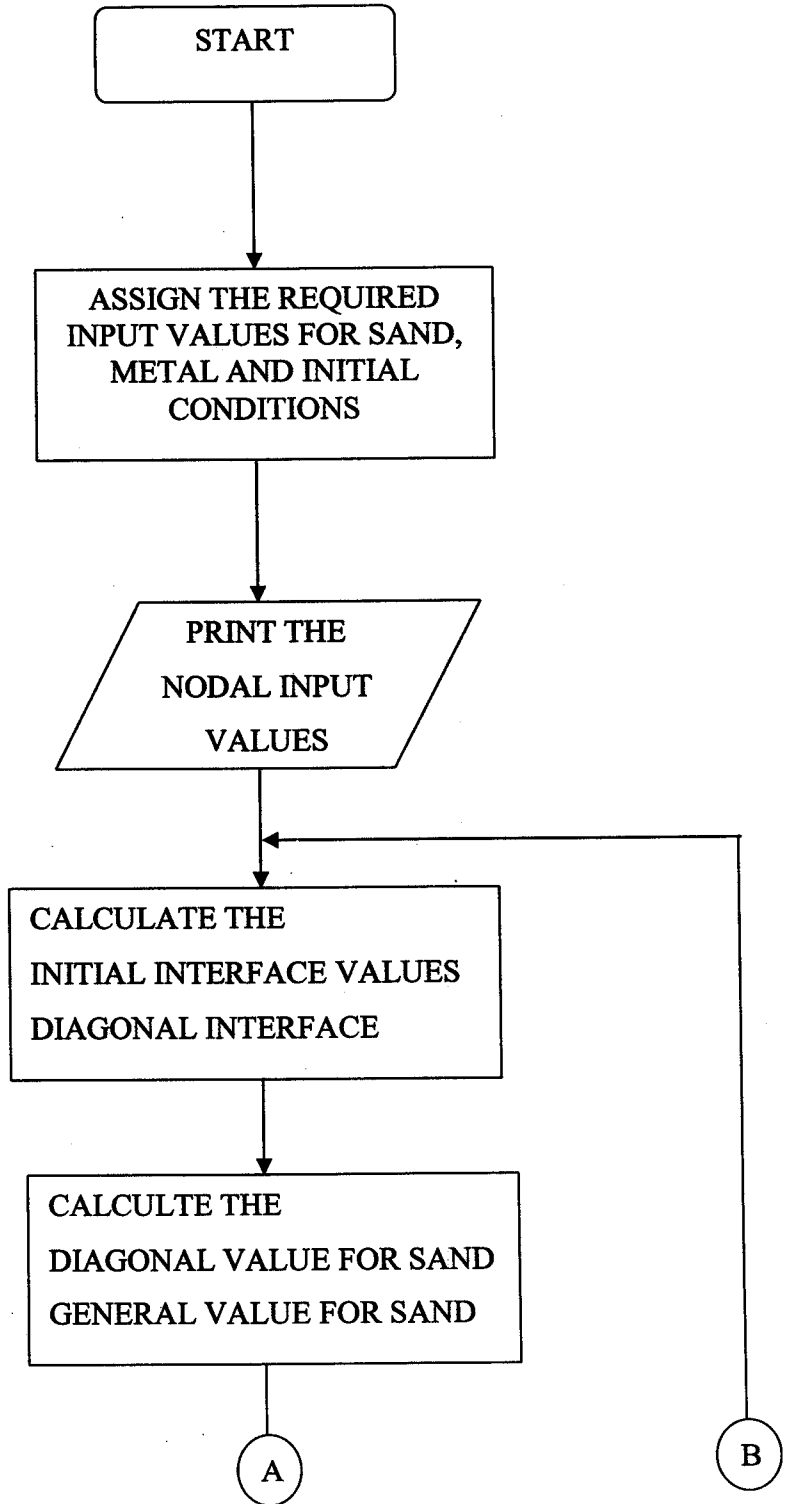
## **7.1 INTRODUCTION**

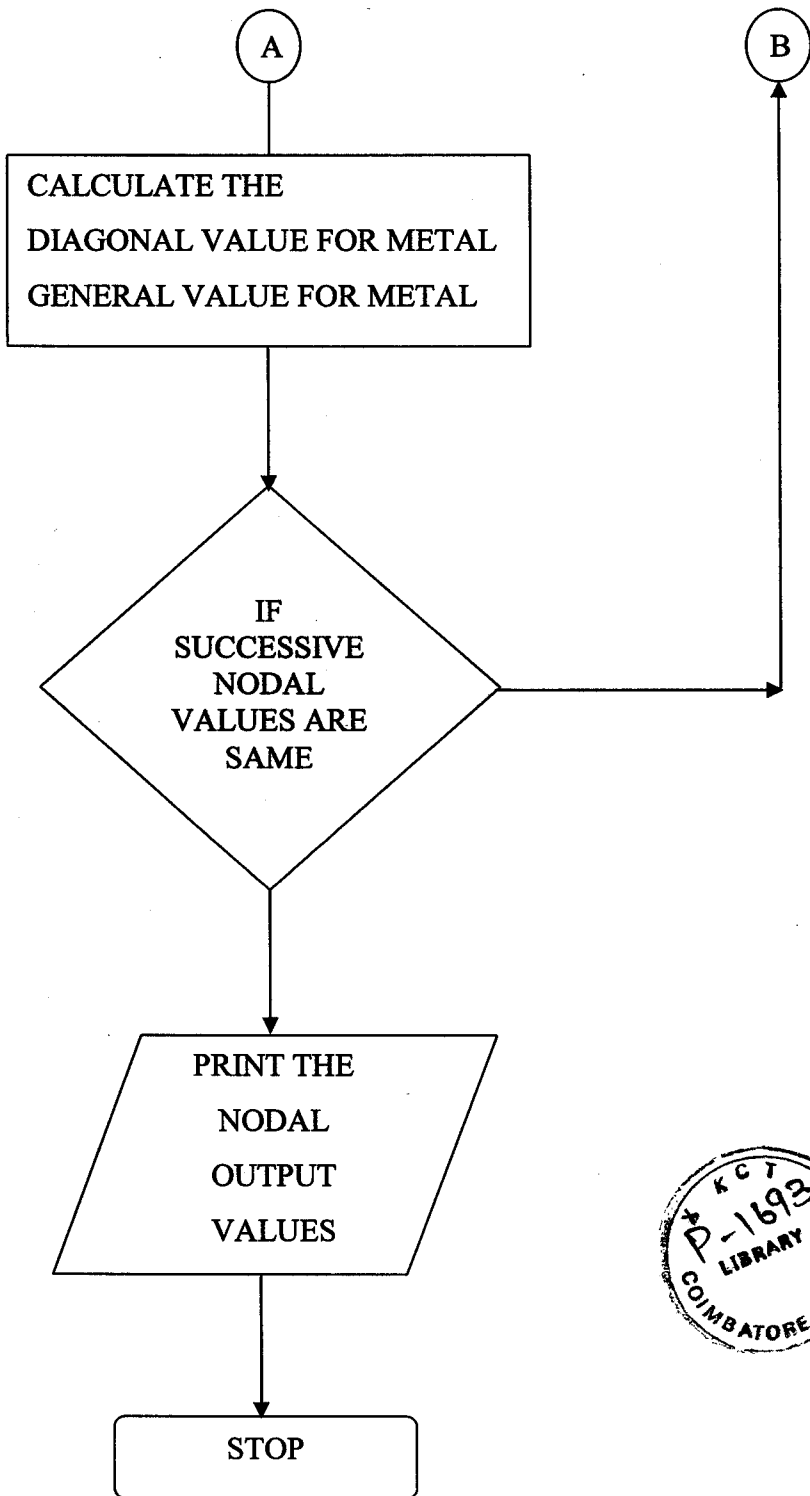
A computer program in C++ language has been developed to perform thermal analysis of two-dimensional solidifying bodies. Using this program the analysis can be made at different grid positions at an economical manner, compare to experimental and software results. The essence of C++ is to allow the programmer to comprehend and manage larger, more complex programs. Thermal properties viz. conductivity and specific heat which is a function of temperature were given as input, and the load conditions are specified. The program gives the temperature distribution in the nodes at various time intervals. The C++ code program developed from the mathematical model can be used for determining the solidification rate for a square geometry. The present program could be used for the simulation of solidification to obtain results with acceptable accuracy.

## **7.2 ALGORITHM**

- Step 1: Start the program
- Step 2: Give the input conditions for sand
- Step 3: Give the input conditions for metal
- Step 4: Give the initial temperature of sand and metal
- Step 5: Calculate the initial interface values
- Step 6: Calculate the diagonal interface value
- Step 7: Calculate the diagonal value for sand
- Step 8: Calculate the general value for sand
- Step 9: Calculate the diagonal value for metal
- Step 10: Calculate the general value for metal
- Step 11: print the nodal input values
- Step 12: Repeat the steps from 5 to 10 for any one  
of successive node values are same
- Step 13: print the nodal output values
- Step 14: stop the program

### 7.3 FLOW CHART











# *Chapter 8*

*Results and Discussions*

The results from Ansys 8.0, mathematical model and the experimental literature report are compared. The output is the graph drawn between temperature and time at different grid positions. The results at particular grid of locations in metal, sand, and interface are represented in graphical form. It could be inferred that as the number of elements were increased, solution approaches the accurate value. The reduction in time taken to solidification in the predictions of ANSYS could be attributed to non-incorporation of thermal resistant between casting and mould. There is slight deviation in temperature values in the metal, interface and sand region as shown in the Figures 8.1, 8.2, 8.3.

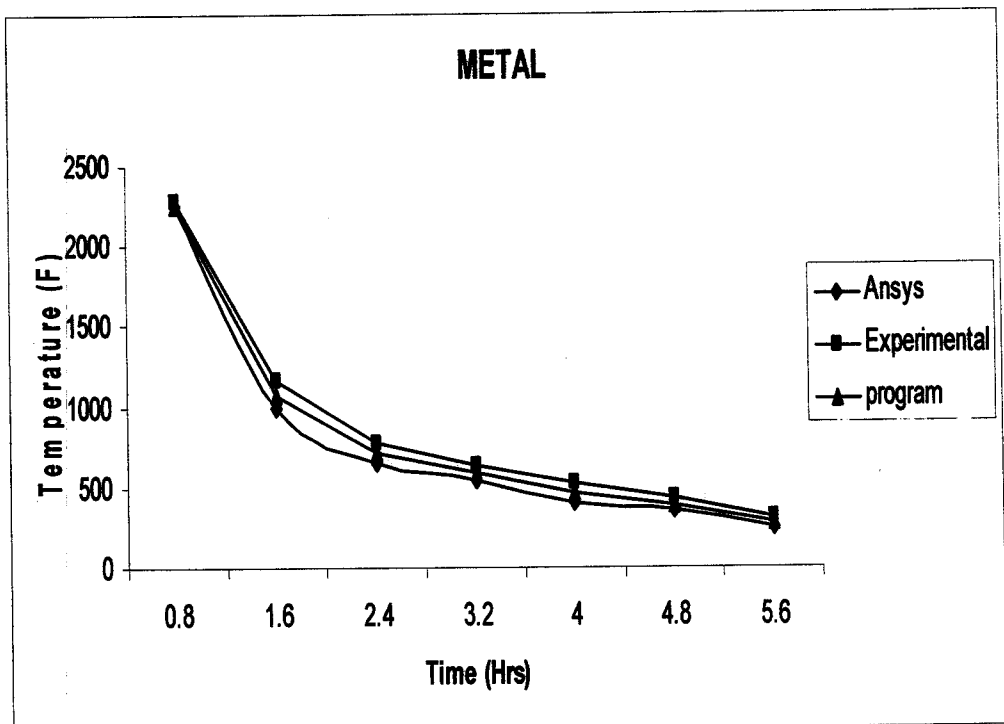


**FIGURE 8.1 TEMPERATURE DISTRIBUTIONS IN METAL**

The initial temperature of the molten metal is considered as 2350 °F and sand is 80 °F . There is not much difference in variation of temperature with respect to time for metal and interface positions. When the molten metal enters the

mould the temperature starts reducing as the surrounding temperature is 80 °F. At 0.8 hrs the temperature decreases to 1000°F.

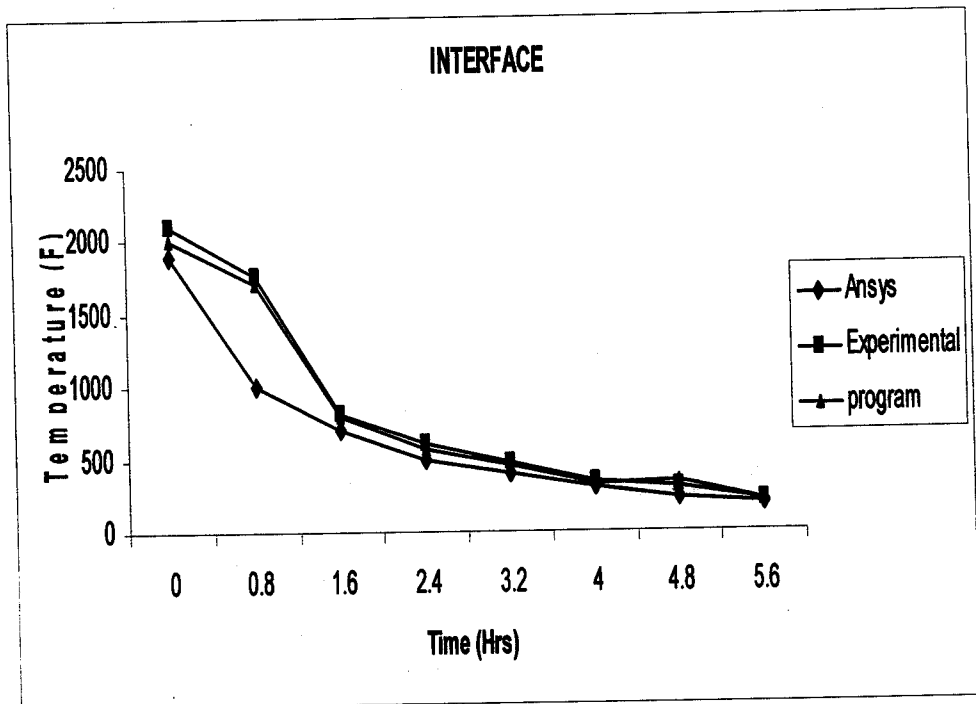


**FIGURE 8.2 TEMPERATURE DISTRIBUTIONS IN INTERFACE REGION**

The interface temperature reaches to 1900 °F when the molten metal is poured into the mould. At 5.5 hrs the temperature of the interface region reduces to 200 °F. Initially the ansys result value drops quicker as compared to experimental and program values.

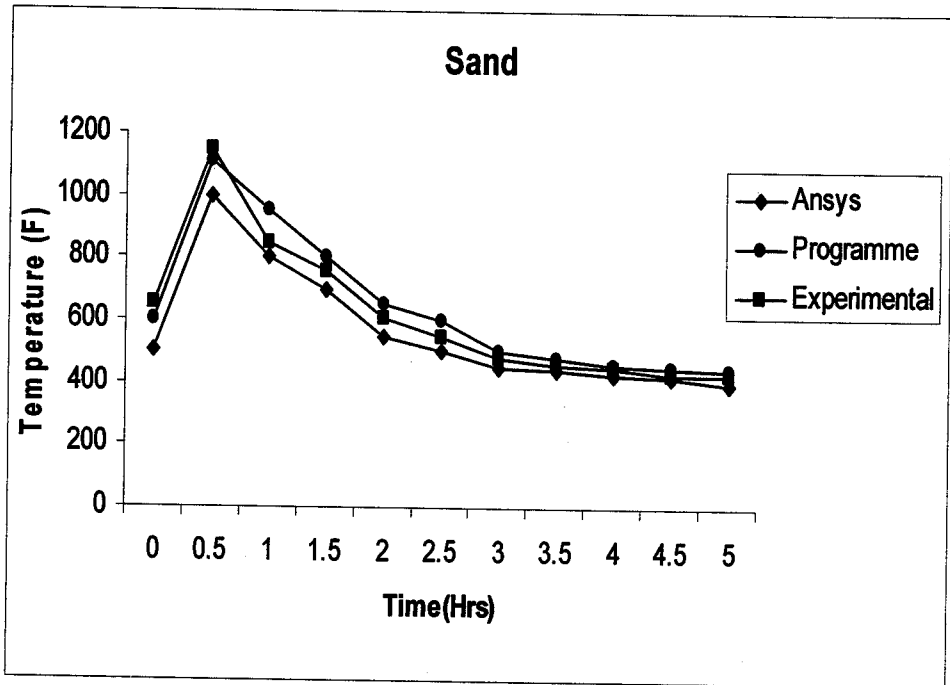


**FIGURE 8.3 TEMPERATURE DISTRIBUTIONS IN SAND**

The node near the interface region has the highest temperature and the value reduces gradually as the node considered is apart from the interface region. The node S1 is near the interface region, which has the initial temperature as 1000 °F, and further increases to 1400 °F and starts stable after 2 hrs reaching 550 °F. Generally the temperature in sand region increases and attain the stable condition and decreases slowly. The results obtain from Ansys, journal and program are similar and there is slight deviation in the values.

# *Chapter 9*

*Conclusions*

In this paper, a C++ code is developed for the simulation of casting solidification. The program can perform two dimensional heat transfer analysis for non-linear transient cases. The program gives the temperature distribution in the nodes at various time intervals. The results obtain from ansys, literature (experimental) and the program are similar, so the developed C++ code program from the mathematical model can be used for determining the solidification rate for a square geometry. The present program could be used for the simulation of solidification to obtain results with acceptable accuracy. Using this program the analysis can be made at different grid positions at an economical manner, compared to experimental and software results. From realistic considerations, the experimental routes are always better for design and development of mold and for arriving at the optimum process parameters, but it is costly and time consuming and may be impossible in some cases. But a computer simulation of the whole process is a convenient way of design of mold and analyzing the effect of various parameters. Solidification rate can be predicted and the type of structure at different grid points can be found from the temperature versus time graph.

*Appendix*



```
#include <iostream.h>
#include <fstream.h>
#include <stdio.h>
#include <conio.h>
#include <stdlib.h>
void main()
{
clrscr();
int n,temp=0,i,j;
int a[25][25]={0};
ofstream out("outmould.txt");
if (! out)
{
cout<<" Cannot open the file";
exit(0);
}
n=21;
for(i=0;i<n;i++)
for(j=i;j<n;j++)
a[i][j]=80;
for(i=14;i<n;i++)
for(j=i;j<n;j++)
a[i][j]=2350;
for(j=13;j<n;j++)
a[13][j]=1530;
a[13][13]=1200;

for(i=0;i<n;i++)
{
out<<"\n\n";
cout<<"\n";
for(j=0;j<n;j++)
{
```

```

{
out.width(5);
out<<"  ";
}
else
{
out.width(5);
out<<a[i][j];
}
if(a[i][j]==0)
{
cout.width(5);
cout<<"  ";
}
else
{
cout.width(5);
cout<<a[i][j];
}
}
}
out<<"\n";
getch();
temp=500;
do{
for(i=12;i>0;i--)
{
for(j=i;j<n-1;j++)
{
if(i==j)
{
a[i][j]=(0.128*((1.8*a[i-1][j]) + (60.9*a[i][j+1]) - (62.7*a[i][j]))) + a[i][j];
}
}
}
}
}

```

```

{
a[i][j]=(0.1167*(a[i+1][j]+a[i-1][j]+a[i][j+1]+a[i][j-1]-(4*a[i][j]))) +a[i][j];
}
if(a[i][j]<80)
a[i][j]=80;
}
}
for(i=14;i<20;i++)
{
for(j=i;j<20;j++)
{
if(i==j)
{
a[i][j]=(0.128*((1.8*a[i-1][j]) + (60.9*a[i][j+1]) - (62.7*a[i][j]))) +a[i][j];
}
else if(i<j)
{
a[i][j]=(.24886*(a[i+1][j]+a[i-1][j]+a[i][j+1]+a[i][j-1]-(4*a[i][j]))) +a[i][j];
}
}
}
temp--;
}
while(temp>0);
cout<<"\n\n";
for(i=0;i<n;i++)
{
out<<"\n\n";
cout<<"\n";
for(j=0;j<n;j++)
{
if(a[i][j]==0)

```

```
out<<" ";
cout.width(5);
cout<<" ";
}
else
{
out.width(5);
out<<a[i][j];
cout.width(5);
cout<<a[i][j];
}
}
}
getch();
}
```

## *References*

- 1) Hacı Mehmet Sahin., Kadir Kocatepe., Ramazan Kayyky, and Neset Akar. (2006), Determination of unidirectional heat transfer coefficient during unsteady-state solidification at metal casting–chill interface, *Energy Conversion and Management* , pp. 19-34.
- 2) Majchrzaka, E. and Szopa, R. (2001), Analysis of thermal processes in solidifying casting using the combined variant of the BEM, *Journal of Materials Processing Technology* , pp.126-132.
- 3) Majchrzaka, E. and Mendakiewicz, J. (1995), Numerical Analysis of Cast Iron Solidification Process, *Journal of Materials Processing Technology* , pp. 285-292.
- 4) Santos, C.A., Spim, J.A. and Garcia, A. (2005), Modeling of solidification in twin-roll strip casting, *Journal of Materials Processing Technology* , pp. 33-39.
- 5) Sulaiman., S. and Hamouda., A.M.S. (2004), Modelling and experimental investigation of solidification process in sand casting, *Journal of Materials Processing Technology* , pp. 1723-1726.
- 6) Venkatesan, A., Gopinath, V.M. and Rajadurai, A. (2005), Simulation of casting solidification and its grain structure prediction using FEM, *Journal of Materials Processing Technology* , pp.10-15.
- 7) Yimin Ruan., Joshua C. Liu. and Owen Richmond. (1993), A deforming finite element method for analysis of alloy solidification problems , *Finite Elements in Analysis and Design* , pp. 49-63.
- 8) Yu-Fang Chiu., Ying-Ling Tsai. and Weng-Sing Hwang. (2003), Mathematical modeling for the solidification heat-transfer phenomena during the reflow process of lead–tin alloy solder joint in electronics packaging , *Applied Mathematical Modeling* , pp. 565–579.
- 9) Zhao, J.Z., Drees, S. and Ratke, L. (2000), Strip casting of Al–Pb alloys - a numerical analysis , *Materials Science and Engineering* , pp. 262-269.